SSC-232

The Superconducting Super Collider

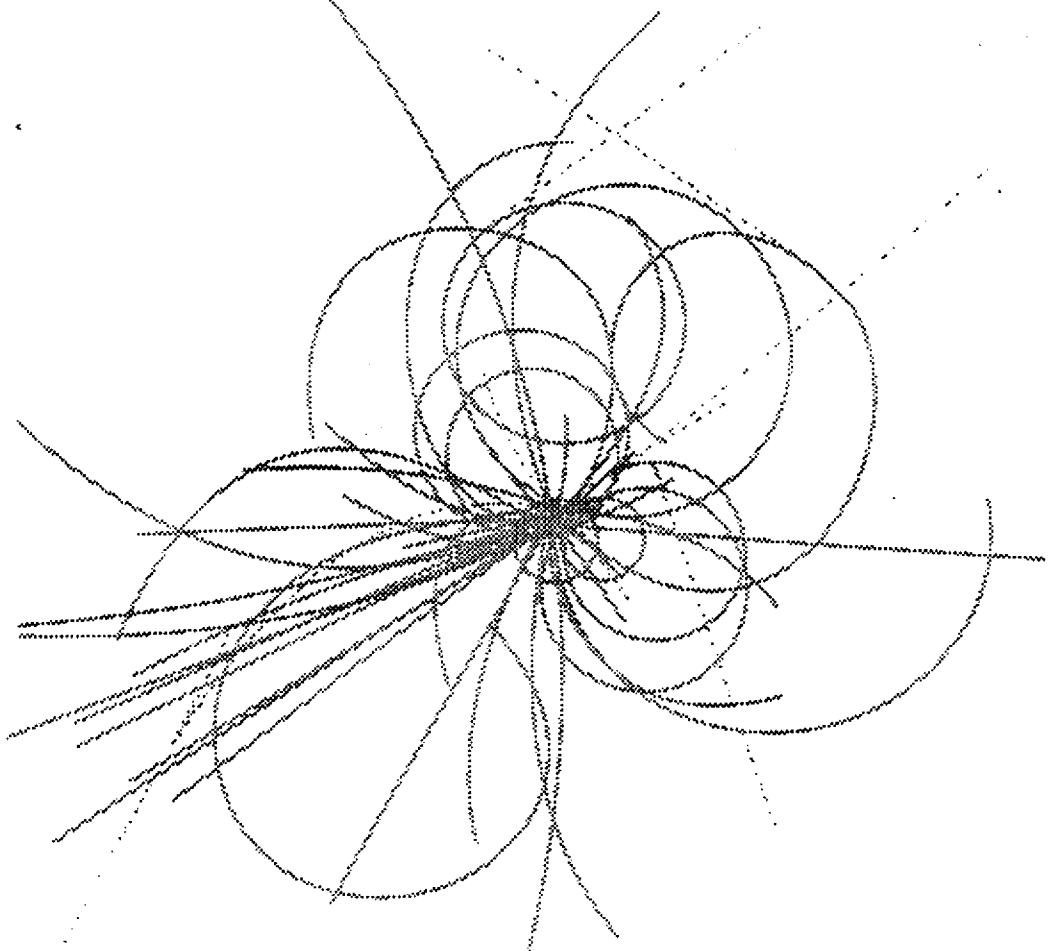

Analytical Calculations of Smear and Tune Shift

J. Bengtsson and J. Irwin

SSC Laboratory

February 1990

SSC-232

ANALYTICAL CALCULATIONS OF SMEAR AND TUNE SHIFT

J. BENGTSSON* AND J. IRWIN†

Superconducting Super Collider Laboratory‡

Dallas, TX 75237

February 1990

* Present address: Lawrence Berkeley Laboratory, One Cyclotron Road, Berkeley, CA 94720

† Present address: Stanford Linear Accelerator Center, P.O. Box 4349, Stanford, CA 94309

‡ Operated by Universities Research Association, Inc. under contract with the U.S. Department of Energy.

Analytical Calculations of Smear and Tune Shift

J. BENGTSSON* AND J. IRWIN†
Superconducting Super Collider Laboratory
Dallas, TX 75237

February 1990

Abstract

We have applied and generalized the Lie algebraic formalism developed by E. Forest to calculate smear and tune shifts due to random and systematic multipole errors for the SSC. In particular, we have calculated smear to the first order in the multipole strength, and tune shifts to the second order. Systematic errors up to octupoles, random errors up to decapoles, and feed-down effects due to closed orbit distortions have been included. For random errors the spread of the smear for an ensemble of accelerators has also been calculated.

The analytical results have been compared with extensive tracking results (averages over 100 seeds have been used for random errors). A histogram of the smear is presented. By Fourier analyzing the tracking results, we have been able to isolate and compare contributions to the smear from different multipoles.

Calculations have been done to study the performance of candidates for the SSC lattice with 4, 5 or 6 dipoles per half cell, 1 or 2 TeV injection energy, and 4 or 5 cm magnet aperture. The improvement obtained by correcting the systematic multipole errors have also been included.

* Present address: Lawrence Berkeley Laboratory, One Cyclotron Road, Berkeley, CA 94720

† Present address: Stanford Linear Accelerator Center, P.O. Box 4349, Stanford, CA 94309

Contents

1. Introduction

Early in the design process for the SSC, the concepts of tune shift and smear were chosen as first order measures of merit of machine designs. Smear was to be a measure of departure from linearity. It has been used extensively by the SSC Central Design Group recently in comparing various systematic multipole error correction schemes. [1, 2] The intention of the concept is clear. Unfortunately, several different quantitative definitions of this term have appeared in the literature. Recently, Furman and Peggs [3] addressed this problem and have suggested a convention for the use of this word which we will follow in this paper.

E. Forest [4] pointed out that tune shifts and smear could be easily calculated from generators that appear in the Lie algebraic analysis of one-turn maps. Other analytical methods have been reported. [5, 6] In this paper, we follow the approach of E. Forest and extend his results in the following ways:

i) We include random decapole errors in the dipole magnets and show that indeed their contribution to the smear is negligible.

ii) We derive analytical expressions for the spread of the smear for an ensemble of machines with specified rms magnet errors.

iii) We derive expressions for the smear in the presence of closed orbit distortions (from dipole field errors, quadrupole misalignment, and beam position monitor (bpm) displacement errors).

iv) We compare our numerical results for the average smear and the spread of the smear with extensive tracking results, using values obtained from 100 different random seeds in the case of random multipoles for the SSC lattice. We are, therefore, also able to present a histogram of the smear.

v) We are able, by Fourier analysis of the tracking data, to isolate and compare contributions to the smear from different multipoles.

vi) We analyze and compute the first and the second order contributions of systematic sextupoles and octupoles to tune shifts.

As a result of this work we can make the following claims:

i) At important amplitudes, the analytical expressions adequately reproduce in detail the average smear, the spread of the smear, and tune shifts derived from tracking. Thus, one can with confidence use analytical techniques to study a wide variety of operating points and lattice configurations. Computation times for each working point are reduced from hours on the CRAY (needed to obtain results with good statistical significance) to seconds on the VAX.

ii) The contributions of various multipoles and closed orbit errors and dependence on amplitude, momentum, and working tune are now clear and the meaning of smear is transparent.

iii) The spread in smear values is typically 40% of its average value. This fact is significant in assessing the confidence that a specified set of parameters will yield the desired linearity. The need for an additional specification, such as long-term dynamic aperture (with modulation included) is clear, and one will want to do long-term tracking for a set of seeds for selected working points.

2. Estimates of Smear and Tune Shifts

2.1 The Definition of Smear

We take the point of view that smear is to be a measure of machine nonlinearity. Under circumstances where quadrupole and skew-quadrupole errors are present, or where a non-zero closed orbit results in feed-down to produce quadrupole and skew-quadrupole errors, we analyze the resultant linear lattice to obtain linear eigensolutions and describe the motion by reference to their respective eigen-amplitudes and eigen-actions. We then follow the recommendations of Ref. [3] and define the smear $S(A_1)$ and $S(A_2)$ of the eigen-actions A_1

and A_2. When there is no linear coupling, we have

$$S_x \equiv \frac{\sqrt{\overline{\Delta A_x^2}}}{\overline{A}_x} \approx \frac{\sqrt{\overline{\Delta J_x^2}}}{2\overline{J}_x}, \qquad \text{if} \quad \Delta J_x \ll J_x \tag{2.1}$$

where A_x is the horizontal betatron amplitude and $\overline{A}_x$ the average. For random errors, we will calculate the averages over an ensemble of accelerators. For computation, we will use the following average

$$< S_x^2 >_{\text{seeds}} \equiv \frac{< \overline{\Delta J_x^2} >_{\text{seeds}}}{4\overline{J}_x^2} \tag{2.2}$$

and for the σ

$$\sigma_{S_x^2} \equiv \frac{\sqrt{< \overline{\Delta J_x^2}^2 - < \overline{\Delta J_x^2} >_{\text{seeds}}^2 >_{\text{seeds}}}}{4\overline{J}_x^2} \tag{2.3}$$

To first order in the multipoles strength, $\overline{J}_x$ may be replaced by J_x. Similar expression holds for the vertical plane. For comparison reasons, the square root of these quantities will be presented.

2.2 Sources of Smear and Tune Shifts

With the exception of random errors, we assume that the lattice is a repetition of identical cells. We wish to find the tune shifts and smear from chromaticity sextupoles, errors in dipole magnets, and misalignment errors of the main quadrupoles. Some of these contributions are the same for each cell, namely from the chromaticity sextupoles, and from the systematic errors in the dipole magnets. Some vary randomly from cell to cell, namely the contribution from the random multipole errors in the dipole magnets, and the misalignment errors. The random misalignment errors of the quadrupoles contribute to a random closed orbit in the dipoles and chromaticity sextupoles, and in this way produce random perturbations.

Since a tolerable design must have both tiny tune shifts and small smear within the usable aperture, it follows quite simply that the machine may be regarded as basically linear, and departures from linearity may be introduced as perturbations.

For evaluating systematic perturbations it is sufficient to limit the analysis to one cell. Clearly, the tune shift of the machine will be equal to the tune shift of one cell times the number of cells. On the other hand, the smear of the full machine will be identical to that for one cell. This is clear if one notes that smear measures the departure from linear orbits, and a one-cell machine is indeed the endless iteration of identical cells. The smear measured in the second cell of a two-cell machine must then be identical to that in the first cell, and no different than the smear measured in a one-cell machine. To obtain a low smear per cell, one needs to choose a working point so that the phase advance per cell is not near a resonance. This choice of tune implies that systematic errors will contribute importantly to tune shifts but little to smear.

On the other hand, for the random errors the full lattice has to be studied. If we consider amplitude resonances

$$n_x \nu_x + n_y \nu_y = p\,, \qquad n_x\,, n_y\,, p = \text{integer} \quad , \tag{2.4}$$

the statement of the previous paragraph implies that the systematic errors will only excite resonances for which the harmonic P is equal to 0 or the number of cells (due to the symmetry of the lattice). For the random errors, many more resonances can contribute to the smear. The tune shifts remain small since the random perturbations of the phase fluctuate around zero from cell to cell.

Since the tune shift is an average over many turns of the phase shift per turn, it can be equivalently regarded as an average over initial phase. It follows that the first order "odd" multipoles, such as sextupoles and decapoles, cannot contribute to tune shift. This fortunate circumstance means that the tolerances on the sextupole can be loosened. However, second order perturbations then

come in to play. Hence, second order contributions to tune shift from sextupoles must be computed. All other perturbations for tune shift and smear can be adequately calculated from first-order perturbation theory.

2.3 Estimates of Smear and Tune Shifts

We begin by assuming that the linear lattice has been analyzed, that coupling is negligible, and that the solution to the linear motion is given by the usual Floquet solution [7]

$$x(s) = \sqrt{2\beta_x(s)J_x}\cos[\theta_x + \phi_x(s)] \tag{2.5}$$

where

$$\phi_x(s) \equiv \int_0^s \frac{d\tau}{\beta_x(\tau)} \quad . \tag{2.6}$$

J_x is the invariant action associated with the x-degree of freedom ($2J_x$ is the Courant–Snyder invariant), θ_x the initial phase, and β_x(s) the beta function. It follows that

$$x' = -\sqrt{\frac{2J_x}{\beta_x(s)}}\{\sin[\theta_x + \phi_x(s)] + \alpha_x(s)\cos[\theta_x(s) + \phi_x(s)]\} \tag{2.7}$$

where

$$\alpha_x(s) \equiv -\frac{1}{2}\beta_x'(s) \quad . \tag{2.8}$$

Then the action and the initial phase are given by the values of x and x' through the equations

$$\begin{aligned} J_x &= \frac{1}{2\beta_x}\left\{x^2 + [\beta_x(s)x' + \alpha_x(s)x]^2\right\} \\ \theta_x &= -\arctan\left[\frac{\beta_x(s)x' + \alpha_x(s)x}{x}\right] - \phi_x(s) \end{aligned} \tag{2.9}$$

To first order, the change in action and the change in phase produced by a small change in x' is then given by

$$\Delta J_x = [\beta_x(s)x' + \alpha_x(s)x]\Delta x' \,, \qquad \Delta\theta_x = -\frac{x}{2J_x}\Delta x' \quad . \tag{2.10}$$

We note that

$$\beta_x(s)x' + \alpha_x(s)x = -\sqrt{2\beta_x(s)J_x}\,\sin[\theta_x + \phi_x(s)] = \frac{\partial x(s)}{\partial\theta_x}\,, \qquad \frac{x(s)}{2J_x} = \frac{\partial x(s)}{\partial J_x} \tag{2.11}$$

so that if the kick $\Delta x'$ can be given in terms of the derivative of a potential function through

$$\Delta x' = -\frac{\partial V(x,y)}{\partial x}\,, \qquad \Delta y' = -\frac{\partial V(x,y)}{\partial y} \quad , \tag{2.12}$$

then we can write Eqs. (2.10) as

$$\Delta J_x = -\frac{\partial V}{\partial\theta_x}\,, \qquad \Delta\theta_x = \frac{\partial V}{\partial J_x} \quad , \tag{2.13}$$

where now $V(x,y)$ is expressed in terms of action-angle variables by writing x and y in terms of action-angle variables. Eqs. (2.13) are reminiscent of Hamilton' equations of motion if interpreted as giving the additional change in J and θ from a perturbing term V in the Hamiltonian. [8, 9] We will come back to this theme in Chapter 3.

Let us first show that indeed there exists such a V for the kicks from magnetic multipoles which we are considering. Indeed, the potential V is proportional to the longitudinal component of the magnetic vector potential, A_s. Since when we neglect end effects there are only transverse components to the magnetic field, the fields may then be expressed as the derivative of A_s. From $\mathbf{B} = \nabla \times \mathbf{A}$, we

have

$$B_x = \frac{\partial A_s}{\partial y}, \qquad B_y = -\frac{\partial A_s}{\partial x} \quad . \tag{2.14}$$

The kick from the magnetic field is given by $\int \mathbf{F} dt$, where $\mathbf{F} = q\mathbf{v} \times \mathbf{B}$. Thus,

$$\Delta x' = \frac{\Delta p_x}{p_0} = -\frac{qLB_y}{p_0}, \qquad \Delta y' = \frac{qLB_x}{p_0} \quad . \tag{2.15}$$

Hence

$$\Delta x' = \frac{qL}{p_0}\frac{\partial A_s}{\partial x}, \qquad \Delta y' = \frac{qL}{p_0}\frac{\partial A_s}{\partial y} \quad , \tag{2.16}$$

from which we may deduce that

$$V(x,y) = -\frac{qL}{p_0} A_s(x,y) \quad . \tag{2.17}$$

The first order expressions for phase shift and smear can now be easily found. The tune shift is the phase advance (divided by 2π) per turn averaged over many turns. The action variables are approximately constant, so the average over turns can be taken as an average over initial phase angle. Thus,

$$2\pi\Delta\nu_x = \langle \Delta\theta_x \rangle_\theta = < \sum_k \frac{\partial V_k}{\partial J_x} >_\theta \quad . \tag{2.18}$$

The sum over k indicates the sum over multipoles in the lattice. To find the smear requires a bit more thought. The changes in J that are given by Eqs. (2.13) result in a distortion of the phase space surfaces for the system. Letting $J_x(\theta)$ and $J_y(\theta)$ denote the phase space surface, then Eqs. (2.13) imply

$$J_x(\theta_x + 2\pi\nu_x, \theta_y + 2\pi\nu_y) - J_x(\theta_x, \theta_y) = \Delta J_x(\theta_x, \theta_y) = -\sum_k \frac{\partial V_k}{\partial \theta_x} \quad . \tag{2.19}$$

If we define an operator, R, that takes any function of (θ_x, θ_y) into the same function evaluated at $(\theta_x + 2\pi\nu_x, \theta_y + 2\pi\nu_y)$, then Eq. (2.19) may be written

$$(R-1)J_x(\theta_x, \theta_y) = -\sum_k \frac{\partial V_k}{\partial \theta_x} \quad . \tag{2.20}$$

Formally this may be solved in the form

$$J_x(\theta_x,\theta_y) = \overline{J}_x - \frac{1}{R-1}\sum_k \frac{\partial V_k}{\partial \theta_x} \quad , \tag{2.21}$$

where $1/(R-1)$ is the inverse operator to $R-1$. Since the V_k are polynomial functions in x and y, and hence in $\cos\theta_x$, $\sin\theta_x$, $\cos\theta_y$ and $\sin\theta_y$, it follows that V_k can be written as a polynomial in $\exp(\pm in_x\theta_x)\exp(\pm in_y\theta_y)$. $R-1$ operating on such a term yields a complex number times the original function. Hence, $1/(R-1)$ is also well defined on such monomials, and by extension, on the polynomial V_k, assuming no monomials with $n_x = n_y = 0$ occur in the decomposition. The smear is the rms value of ΔJ_x divided by two times its average value (Eq. (2.1)), hence,

$$S(A_x) = \frac{1}{2\overline{J}_x}\left[\left\langle\left(\frac{1}{R-1}\sum_k \frac{\partial V_k}{\partial \theta_x}\right)^2\right\rangle_\theta\right]^{1/2} \quad . \tag{2.22}$$

As an example, we will calculate (to first order) tune shifts for random normal octupoles and smear for random normal sextupoles. First order tune shift for sextupoles is zero since the θ average of $x^{n_x}y^{n_y}$ is zero if n_x, n_y, or n_x+n_y is odd. The magnetic multipoles in the SSC dipoles are usually parametrized through the formula[10]

$$B_y + iB_x = B_0\sum_{n=0}^{\infty}(b_n + ia_n)(x+iy)^n \quad , \tag{2.23}$$

where B_0 is the design bending field and b_n, a_n are the normal and skew multipole strengths with the dimension $\mathrm{m}^{-\mathrm{n}}$. It is customary to quote a_n and b_n in units of 10^{-4} measured at a reference radius $r_0 = 10^{-2}\,\mathrm{m}$. If we write

$$B_y + iB_x = \hat{B}_0\sum_{n=0}^{\infty}(b_n + ia_n)\left(\frac{x+iy}{r_0}\right)^n \quad , \qquad \hat{B}_0 \equiv B_0\cdot 10^{-4} \quad , \tag{2.24}$$

then for the SSC these parameters range from 0.1 to 10. (See Table S-1[11]). Given Eq. (2.23) for the magnetic field, it follows that the potential function V

is given by

$$V = r_0\hat{\theta}_d Re\sum_{n=0}^{\infty}\frac{1}{n+1}(\hat{b}_n + i\hat{a}_n)\left(\frac{x+iy}{r_0}\right)^{n+1} \quad , \tag{2.25}$$

where $\hat{\theta}_d \equiv qLB_0/p_0 \cdot 10^{-4} = L/\rho \cdot 10^{-4}$ is 10^{-4} times the bend angle of the reference orbit in the dipole magnets, about $2\pi/4000 \cdot 10^{-4}$. Hence, the potential for the normal octupole located at $s = s_k$, is

$$V_k^{3N} = r_0\hat{\theta}_d\hat{b}_{3k}\frac{1}{4r_0^4}(x_k^4 - 6x_k^2y_k^2 + y_k^4) \quad . \tag{2.26}$$

A simple way to find the averages over θ is to write the cosine of Eq. (2.5) as a sum of complex exponentials, and use the binomial theorem to extract the θ independent term. For example,

$$< \cos^4\theta_x >= \frac{3}{8}, \qquad < \cos^2\theta_x >= \frac{1}{2} \tag{2.27}$$

so

$$< V_k^{3N} >= \hat{\theta}_d\hat{b}_{3k}\frac{1}{8r_0^3}\left[3\beta_{xk}^2J_x^2 - 12\beta_{xk}\beta_{yk}J_xJ_y + 3\beta_{yk}^2J_y^2\right] \quad . \tag{2.28}$$

Next we need to sum this quantity over all k. For random octupoles, the strength $\hat{b}_{3k}$ will be $r_k\sigma_{\hat{b}_3}$, where the r_k are normally distributed random numbers with an rms spread of unity. This, in turn, implies that the sum over k when various random seeds are considered, will be

$$\begin{aligned}\sum_k < V_k^{3N} > = r_{\#}\sqrt{N}\hat{\theta}_d\sigma_{\hat{b}3}\frac{1}{8r_0^3}\left[3 < \beta_{xk}^2 > J_x^2 - 12 < \beta_{xk}\beta_{yk} > J_xJ_y\right. \\ \left. +3 < \beta_{yk}^2 > J_y^2\right] \quad .\end{aligned} \tag{2.29}$$

where N is the total number of dipoles, $r_{\#}$ is a random number chosen from a normal distribution of unit width, and the averages of the powers of the beta functions can be taken over any single cell. The derivative of Eq. (2.29) with

respect to J_x or J_y will give 2π times the x and y tune shift, respectively. For example,

$$2\pi\Delta\nu_x = r_{\#}\sqrt{N}\hat{\theta}_d\hat{\sigma}_{b_3}\frac{3}{4r_0^3}\left[<\beta_{xk}^2> J_x - 2<\beta_{xk}\beta_{yk}> J_y\right] \quad . \tag{2.30}$$

To carry this one step further, it is usual to express such a result in terms of the maximum amplitude of oscillation at a point in the arcs where the beta function is maximum; namely, we write $J_x = x_{max}^2/(2\beta_x^{max})$ and $J_y = y_{max}^2/(2\beta_y^{max})$.

$$2\pi\Delta\nu_x = \frac{r_{\#}\sqrt{N}\hat{\theta}_d\hat{\sigma}_{b3}}{2\beta_x^{max}}\frac{3}{4r_0^3}\left[<\beta_{xk}^2> x_{max}^2 - 2<\beta_{xk}\beta_{yk}> y_{max}^2\right] \quad , \tag{2.31}$$

where $N = 4000\,, \hat{\theta}_d = 2\pi/4000\cdot 10^{-4}\,, \sigma_{\hat{b}3} = 0.3\,,\ \beta_x^{max} \approx \beta_y^{max} \approx 360\,\mathrm{m}\,,\ <\beta_{xk}^2> = 4.3\times 10^4\,\mathrm{m}^2$, and $<\beta_{xk}\beta_{yk}> = 2.8\times 10^4\,\mathrm{m}^2$. [12] The order of magnitude here is given by the combination of factors:

$$\begin{aligned}\Delta\nu_x &\approx \sqrt{N}\frac{\hat{\theta}_d}{2\pi}\sigma_{\hat{b}_3}\frac{<\beta_x>}{r_0}\frac{x^2}{r_0^2} \\ &\approx 63\cdot 10^{-4}\cdot\frac{1}{4000}\cdot 0.3\cdot 1.2\cdot 10^4(0.6)^2 \approx 0.007\end{aligned} \quad . \tag{2.32}$$

More precisely

$$\begin{pmatrix}\Delta\nu_x\\ \Delta\nu_y\end{pmatrix} = r_{\#}\begin{pmatrix}0.0041 & -0.0052\\ -0.0052 & 0.0040\end{pmatrix}\begin{pmatrix}x_{max}^2/r_0^2\\ y_{max}^2/r_0^2\end{pmatrix} \quad . \tag{2.33}$$

We see here that the first order tune shifts from the random octupoles are normally distributed.

To calculate the smear from sextupoles, we begin with Eq. (2.22). For the normal sextupole, we have

$$V_k^{2N} = \hat{\theta}_d\hat{b}_{2k}\frac{1}{3r_0^2}(x_k^3 - 3x_k y_k^2) \quad . \tag{2.34}$$

Next, we expand x_k, x_k^3, and y_k^2 in terms of complex exponentials. For example,

$$x_k^3 = \left(\frac{\beta_{xk} J_x}{2}\right)^{3/2} \left[e^{3i(\theta_x+\phi_{xk})} + 3e^{i(\theta_x+\phi_{xk})} + cc\right] \quad , \tag{2.35}$$

where cc stands for the complex conjugate. The operator $1/(R-1)$ and the derivative with respect to θ_x on this term give

$$\frac{1}{R-1}\frac{\partial x_k^3}{\partial \theta_x} = \left(\frac{\beta_{xk} J_x}{2}\right)^{3/2} \left[\frac{3ie^{i3(\theta_x+\phi_{xk})}}{e^{i2\pi 3\nu_x}-1} + \frac{3ie^{i(\theta_x+\phi_{xk})}}{e^{i2\pi\nu_x}-1} + cc\right] \quad . \tag{2.36}$$

The operations must be performed for $-x_k y_k^2$. Then these are added, summed over k, multiplied times itself (summed over j), averaged over $\boldsymbol{\theta}$, and finally the square root is taken to get the smear. Instead of proceeding further with this example, we write down a more general expression

$$\begin{aligned}\Delta J_x(\theta) = J_x(\theta) - \overline{J_x} &= \frac{1}{R-1}\sum_k \frac{\partial V_k}{\partial \theta_x} = \frac{1}{R-1}\sum_{k,n_x\geq 0,n_y} r_k \left(B_{nk} e^{i\mathbf{n}\cdot\boldsymbol{\theta}} + cc\right) \\ &= \sum_{k,n_x\geq 0,n_y} \left(r_k A_{nk} \frac{i n_x e^{i\mathbf{n}\cdot\boldsymbol{\phi k}}}{e^{2\pi \mathbf{n}\cdot\boldsymbol{\nu}}-1} e^{i\mathbf{n}\cdot\boldsymbol{\theta}} + cc\right) \quad .\end{aligned} \tag{2.37}$$

Here, the in_x comes from the derivative with respect to θ_x, the denominator is the $R-1$ factor, the A_{nk} is real and is a polynomial in the beta functions and the action variables. The sum is restricted to $n_x \geq 0$ since the $n_x < 0$ terms then appear in the complex conjugate (cc) terms.

If we square this result and average over $\boldsymbol{\theta}$, we get

$$\begin{aligned}\overline{\Delta J_x^2(\vec{r_\#})} = <\Delta J_x^2(\theta)>_\theta &= \left\langle \left(\frac{1}{R-1}\sum_k \frac{\partial V_k}{\partial \theta_x}\right)^2 \right\rangle_\theta \\ &= \frac{1}{2\pi}\sum_{j,k,n_x\geq 0,n_y} r_j r_k [B_{nj} B_{nk} + cc] \\ &= \frac{1}{2\pi}\sum_{j,k,n_x\geq 0,n_y} r_j r_k A_{nj} A_{nk} n_x^2 \frac{\cos \mathbf{n}\cdot(\boldsymbol{\phi}_j - \boldsymbol{\phi}_k)}{\sin^2 \pi \mathbf{n}\cdot\boldsymbol{\nu}} \quad .\end{aligned} \tag{2.38}$$

Here we see the "resonance denominators" that are important to the smear calculation. If we ask for the average value of the above expression, averaged over random seeds, then only the $j = k$ terms survive, and we get

$$< \overline{\Delta J_x^2(\vec{r_\#})} > = \left\langle \left\langle \frac{1}{R-1} \sum_k \left(\frac{\partial V_k}{\partial \theta_x} \right)^2 \right\rangle_\theta \right\rangle_{\text{seeds}} = \frac{1}{\pi} \sum_{\substack{k,ny \\ nx \geq 0}} B_{nk} B_{nk}$$
$$= \frac{1}{\pi} \sum_{\substack{k,ny \\ nx \geq 0}} A_{nk}^2 n_x^2 \frac{1}{\sin^2(\pi \mathbf{n} \cdot \boldsymbol{\nu})} \quad . \tag{2.39}$$

In addition to this average it is of interest to calculate the spread over random seeds of the expression in Eq. (2.37).

$$< \overline{\Delta J_x^2(\vec{r_\#})}^2 > - < \overline{\Delta J_x^2(\vec{r_\#})} >^2 = \frac{2}{\pi} \sum_{j \neq k} \sum_{\substack{m_x \geq 0 \\ n_x \geq 0 \\ m_y, n_y}} A_{mj} - A_{mk} A_{nj} A_{nk} n_x^2 m_x^2$$
$$\cdot \frac{\cos \mathbf{m} \cdot (\phi_j - \phi_k) \cos \mathbf{n} \cdot (\phi_j - \phi_k)}{\sin^2 \pi \mathbf{m} \cdot \boldsymbol{\nu} \sin^2 \pi \mathbf{n} \cdot \boldsymbol{\nu}} \quad . \tag{2.40}$$

The precise analytic expressions will be presented in Chapter 4.

Taking the specifications in Table S-1, [11] for nonlinear multipole errors present in the dipoles, the principal contributions typically come from the sextupole and the octupole errors. This result depends, of course, on the operating tunes. Higher multipoles are quite negligible.

Since the total integrated length of the quadrupoles is much smaller than the dipoles, the nonlinearities in the quadrupoles give a negligible contribution to the nonlinearity of the machine at injection. For collision optics, the nonlinearities from the interaction region quadrupoles can become dominant. Here we limit our attention to the situation at injection.

Random quadrupole and skew-quadrupole errors in the dipoles do not contribute directly to the smear, but they create a slight randomness in the cell-to-

cell phase advance and beta function. As a result, there is a random contribution to the nonlinear contributions of the systematic dipole multipoles. This arises also when closed orbit errors are present since they give normal and skew quadrupole terms through feed-down.

3. Smear and Tune Shifts from Lie Generators

In this chapter, we derive expressions for smear and tune shift using Lie algebra techniques. It is possible to extend the above results to higher orders, and as an example, we derive the expression for second order tune shift which we need for sextupoles. Additionally, the Lie algebraic formulation affords insight into the quantities we are computing.

3.1 The Exponential Lie Operator

There have been several descriptions of the Lie algebra techniques. [13, 4, 14, 2] We present here the main results with explanatory comments. The exponential Lie operator is written $\exp(:f:)$. It operates on a function space, and is defined by

$$e^{:f:}g = g + [f,g] + \frac{1}{2}[f,[f,g]] + ... \quad , \tag{3.1}$$

where $[f,g]$ is the Poisson bracket of f and g. If $\exp(:f:)$ operates on a coordinate function, then the result

$$x_f = e^{:f:}x = x + [f,x] + \frac{1}{2}[f,[f,x]] + ... \tag{3.2}$$

can be interpreted as the value of the coordinate at a time $t = 1$, expressed as a function of the coordinates at time $t = 0$, for a dynamical system with a Hamiltonian $H = -f$. Since the Poisson bracket viewed as an operator falls into

a class of operators which are derivations (: f : can be viewed as the operator $-d/dt$), it follows that

$$e^{:f:}x^n = x_f^n \tag{3.3}$$

and thus for polynomial functions

$$e^{:f:}g(z) = g\left(e^{:f:}z\right) \tag{3.4}$$

Of special interest is the case where $f(x, p_x, y, p_y)$ is only a function of x and y. Then,

$$x_f = x_i\,, \qquad y_f = y_i\,, \qquad p_{x_f} = p_{x_i} + \frac{\partial f}{\partial x_i}\,, \qquad \text{and} \qquad p_{y_f} = p_{y_i} + \frac{\partial f}{\partial y_i} \tag{3.5}$$

We call this a kick Hamiltonian; it can be an accurate representation of a thin magnetic lens. For the multipole kicks described in Chapter 2, Eq. (2.17),

$$f(x,y) = -V(x,y) = \frac{qL}{p_0}A_s(x,y) \tag{3.6}$$

3.2 The Algebra of Exponential Lie Operators

The operator exp(: f :) interpreted as a map, is necessarily a symplectic map, since it produces a coordinate transformation generated by a Hamiltonian function. Thus these maps may be composed to create an algebra of symplectic maps. Suppose we have two operators

$$z_2 = e^{:f_1(z_1):}z_1\,, \qquad \text{mapping } z_1 \text{ to } z_2 \tag{3.7}$$

and

$$z_3 = e^{:f_2(z_2):}z_2\,, \qquad \text{mapping } z_2 \text{ to } z_3\,, \tag{3.8}$$

then the composition

$$z_3 = e^{:f_2(z_2):}e^{:f_1(z_1):}z_1 = e^{:f_2(z):}z\Big|_{z=e^{:f_1(z_1):}z_1} \tag{3.9}$$

has one exponent expressed in terms of the original variables z_1, and the second exponent expressed as a function of the intermediate variables. A bit of thought

(and doing one simple example) shows that the result is the same as

$$z_3 = e^{:f_1(z_1):} e^{:f_2(z_1):} z_1 \quad . \tag{3.10}$$

Briefly, $f_2(z_1)$ operates on z_1 as if the variable was z_2, and then because of property from Eq. (3.4) above, the operator exp[: $f_1(z_1)$:] changes z_1 everywhere to z_2 (expressed as a function of z_1). This is exactly the composition desired.

Of course, Eq. (3.10) is more convenient and allows us to build a powerful operator algebra. A combination of particular importance is completely analogous to the similarity transformation so familiar in linear matrix algebra

$$e^{:g:} e^{:f:} e^{:-g:} = e^{:e^{:g:} f:} = e^{:f(e^{:g:} z):} \quad . \tag{3.11}$$

Finally, there is a theorem, known as the Campbell-Baker-Hausdorff Theorem, by which a product of two operators may be combined into one

$$e^{:f_2:} e^{:f_1:} = e^{:f:} \quad , \tag{3.12}$$

where f is given by

$$f = f_2 + f_1 + \frac{1}{2}[f_2, f_1] + \frac{1}{12}[f_2, [f_2, f_1]] - [f_2, [f_2, f_1]] - \frac{1}{24}[f_1, [f_2, [f_2, f_1]]] + \ldots \tag{3.13}$$

The remaining terms, involving four or more commutators, become quite numerous and no simple pattern is apparent. In practice, this formula is of interest in those cases where f_1 and f_2 are small, and the series converges rapidly. Fortunately, this is the case for accelerators where nonlinearities are kept as small as possible so that the motion is very close to linear.

3.3 Lie Product Representation of Accelerator Lattices

If we represent our accelerator by a combination of linear elements and nonlinear kicks, then the map for the lattice will be given by an expression of the form

$$\mathcal{M} = M_{N+1} e^{:f_N:} M_N e^{:f_{N-1}:} ... e^{:f_2:} M_2 e^{:f_1:} M_1 \quad , \tag{3.14}$$

where the M_N are linear operators and the $f_n = f_n(x_n, y_n)$ are multipole kicks at the longitudinal coordinate $s = s_n$. According to Eq. (3.10), we may write this product in terms of one set of variables by reversing the order of the products. We then have

$$\mathcal{M} = M_1 e^{:f_1:} M_2 e^{:f_2:} ... e^{:f_{N-1}:} M_N e^{:f_N:} M_{N+1} \quad , \tag{3.15}$$

where all generators are now a function of the same (initial) variable. If we define $\overline{M}_n = M_1 M_2 M_3 ... M_n$, then by inserting identities of the form $M_{n-1} M_n$ into Eq. (3.15), and using the similarity relation, Eq. (3.15), many times we can transform Eq. (3.15) into the form

$$\mathcal{M} = e^{:\overline{M}_1 f_1:} e^{:\overline{M}_2 f_2:} ... e^{:\overline{M}_{N-1} f_{N-1}:} e^{:\overline{M}_N f_N:} \overline{M}_{N+1} \quad . \tag{3.16}$$

The nonlinear kicks have been "rotated" to the front of the lattice. The $\overline{M}_n$ transform the initial variable to the variable at the location of the kick.

In the case that the map is a one-turn map for a circular machine, it is usual to introduce two similarity transformations, one which translates the origin to the fixed point of the map, and the second which transforms the linear part of the map to a block diagonal rotation. If the origin is not a fixed point (one supposes it is close to the fixed point), the fixed point may be found by constructing the inverse to the map, and finding the image of the origin. Then the map

$$\mathrm{T_a} = e^{:\mathbf{a}\cdot\mathbf{z}:} \quad , \tag{3.17}$$

where : $\mathbf{a} \cdot \mathbf{z} := \sum_{ij} a_i J_{ij} z_j$ and J_{ij} is the symplectic form, will map the origin into the fixed point a.

Let us suppose that the map of Eq. (3.16) has been translated if needed, so that it already maps the origin into itself. Let the matrix corresponding to the linear map $\overline{M}_{N+1}$ be $\widehat{M}$. Because $\widehat{M}$ is a symplectic matrix, it is possible to find eigenvalues which, if $\widehat{M}$ is stable, will lie on the unit circle and occur in pairs. Using the eigenvectors corresponding to these eigenvalues, we can construct a similarity transformation $\widehat{A}_0$ with the property

$$\widehat{M} = \widehat{A}_0 \widehat{R} \widehat{A}_0^{-1} \quad , \tag{3.18}$$

where $\widehat{R}$ is a simple block rotation matrix

$$\widehat{R} = \begin{pmatrix} \widehat{R}_x & 0 \\ 0 & \widehat{R}_y \end{pmatrix} , \qquad \widehat{R}_x = \begin{pmatrix} \cos\theta_x & \sin\theta_x \\ -\sin\theta_x & \cos\theta_x \end{pmatrix} \quad . \tag{3.19}$$

We now insert these results into Eq. (3.16), remove the "^", to denote the corresponding Lie operator rather than the matrix, and additionally introduce identities in the form $A_0^{-1}A_0$, so that we can move the A_0^{-1} through the nonlinear kicks. We get

$$\mathcal{M} = A_0^{-1} e^{:A_0\overline{M}_1 f_1:} e^{:A_0\overline{M}_2 f_2:} \ldots e^{:A_0\overline{M}_N f_N:} R A_0 \quad . \tag{3.20}$$

The functions

$$\widetilde{f}_n = A_0 \overline{M}_n f_n = f_n(A_0 \overline{M}_n z) \tag{3.21}$$

are the functions $\overline{f}_n$ written in terms of the eigencoordinates at the longitudinal location $s = s_n$. If there were no coupling present, then, for example,

$$\begin{aligned} x_n &= A_0 \overline{M}_n x \\ &= \sqrt{2\beta_{xn} J_x} \cos(\theta_x + \phi_{xn}) + \eta_{xn}\delta \end{aligned} \quad , \tag{3.22}$$

where β_n , ϕ_n , η_n are the usual beta function, phase advance and linear dispersion function at the point $s = s_n$, and the momentum deviation δ is defined by

$$\delta \equiv \frac{p - p_0}{p_0} \quad , \tag{3.23}$$

where p_0 is the momentum of a reference particle.

At this point, we may drop the overall similarity transformation, A_0, and study the map

$$\widehat{\mathcal{M}} = e^{:\widetilde{f}_1:} e^{:\widetilde{f}_2:} \ldots e^{:\widetilde{f}_N:} R \quad . \tag{3.24}$$

The Campbell-Baker-Hausdorff theorem, Eq. (3.17), can be used to write the result in a particularly simple form

$$\widehat{\mathcal{M}} = e^{:f:} R \quad . \tag{3.25}$$

Of course, f is a generator which, in general, is difficult to find, but the first terms in the perturbation series may be found quite easily, and one may hope that this will be adequate if the $\widetilde{f}_n$ are small. We have

$$f = \sum_{n=1}^{N} \widetilde{f}_n + \sum_{\substack{n \\ m<n}}^{N} [\widetilde{f}_m, \widetilde{f}_n] + \ldots \tag{3.26}$$

3.4 Lie Product Normal Form

We now describe a process which is a generalization of the procedure introduced in Eqs. (2.19) through (2.21). The map of Eq. (3.25) will distort the invariant phase space surfaces around the origin. For small actions these surfaces will be tori, the products of phase space circles in each phase space degree of freedom. As the action increases the invariant surfaces are slightly distorted. As the action increases further, the surfaces become only approximations to the actual motion, and eventually the concept of invariant surface breaks down entirely. We are interested in the regions that have invariant surfaces or approximate invariant surfaces and we would like to find such surfaces. If such surfaces exist, they will form an onion-like structure in phase space, and there will be a map that deforms the tori into these more complicated shapes. Let such a map be noted

by exp(: g :). This map should satisfy an equation of the form

$$\widehat{\mathcal{M}} = e^{:f:} R = e^{:g:} \widetilde{R} e^{-:g:} \quad , \tag{3.27}$$

where $\widetilde{R} = R\exp(: h :)$ is an amplitude dependent rotation in the toroidally structured space. h will be a function of the action variables only. $\widetilde{R}$ contains the information about phase shift with amplitude, the operator exp(: g :) contains the information about the phase space distortion. The operator exp(: g :) will determine the smear. If Eq. (3.27) is indeed a valid equation, then we can move R on the right-hand side to the right by inserting an RR^{-1} on the right, and then use the Campbell-Baker-Hausdorff equation to find

$$\begin{aligned} e^{:f:} R &= e^{:g:} R e^{:h:} e^{:-g:} = e^{:g:} e^{:h:} e^{:-Rg:} R \\ &= e^{:(1-R)g+h-1/2[g,Rg]-1/2[h,(1+R)g]+\cdots} R \end{aligned} \quad . \tag{3.28}$$

Suppose that f is given in the form

$$f = \epsilon f_1 + \epsilon^2 f_2 + \ldots \tag{3.29}$$

and we wish to find a corresponding expression for g and h; namely,

$$\begin{aligned} g &= \epsilon g_1 + \epsilon^2 g_2 + \ldots \\ h &= \epsilon h_1 + \epsilon^2 h_2 + \ldots \end{aligned} \quad . \tag{3.30}$$

Equating terms which are first order in ϵ, we get

$$(1 - R)g_1 + h_1 = f_1 \quad . \tag{3.31}$$

This may be solved uniquely by decomposing f_1 into two parts

$$f_1 = f_1^- + f_1^* \quad , \tag{3.32}$$

where f_1^- is the average of f_1 over phase angle, and $f_1^* = f_1 - f_1^-$ is the remainder. Then we may set

$$h_1 = f_1^- \qquad \text{and} \qquad g_1 = \frac{1}{1-R} f_1^* \quad . \tag{3.33}$$

The operator $1/(1-R)$ is well defined on f_1^* since the terms in f_1, which are independent of angle, have been removed.

Equating terms which are second order in ϵ, we get the equation

$$(1-R)g_2 + h_2 = f_2 + \frac{1}{2}\left[g_1, Rg_1\right] + \frac{1}{2}\left[h_1, (1+R)g_1\right] \quad . \tag{3.34}$$

We proceed exactly as in Eqs. (3.31). There are two simplifications

$$\begin{aligned} \left[h_1, (1+R)g_1\right]^- &= 0 \\ \left[g_1, Rg_1\right] &= \left[\frac{1}{1-R} f_1^*, \frac{R}{1-R} f_1^*\right] = \left[f_1^*, \frac{1}{1-R} f_1^*\right] \end{aligned} \quad . \tag{3.35}$$

The result is

$$\begin{aligned} h_2 &= f_2^- + \frac{1}{2}\left[f_1^*, \frac{1}{1-R} f_1^*\right]^- \\ g_2 &= \frac{1}{1-R} f_2^* + \frac{1}{2}\left[f_1^*, \frac{1}{1-R} f_1^*\right]^* + \frac{1}{2}\left[f_1^-, \frac{1+R}{1-R} f_1^*\right] \end{aligned} \quad . \tag{3.36}$$

This procedure could be continued to higher orders.

3.5 Lie Algebraic Expression for Tune Shift and Smear

There are two sets of phase space angles one can discuss: one set is the original phase angles, the other set is the image of the first set under the map $\exp(:g:)$. (Recall that in "local coordinates" the order of the factors in Eq. (3.27) is reversed.) The same tune shift would result using either set, because a revolution traversed in one set implies a revolution traversed in the other set. The

image of the original space under exp(: g :) we call the Floquet space, and the phase angles in this space the Floquet angles. The Floquet angles are rotated by the operator $\widetilde{R}$. Combining the operator exp(: h :) with the operator $R = \exp(: -\boldsymbol{\mu_0} \cdot \mathbf{J})$, we have

$$\widetilde{R} = e^{:-\boldsymbol{\mu_0}\mathbf{J}+h:} \tag{3.37}$$

and the phase advance per turn is given by

$$\mu_i(\mathbf{J}) = \mu_{0i} - \frac{\partial h}{\partial J_i} \quad . \tag{3.38}$$

The smear can be found by using exp(: g :) to calculate the change in the actions. We have

$$J_i' = e^{:-g:} J_i \quad , \tag{3.39}$$

hence,

$$\Delta J_i = e^{:-g:} J_i - J_i \quad . \tag{3.40}$$

The smear is found by taking the average over the angle of the square of this expression. If we are content with a first-order expression, then

$$\Delta J_i = -\frac{\partial g}{\partial \theta_i} = \frac{1}{R-1}\frac{\partial f_1^*}{\partial \theta_i} \quad , \tag{3.41}$$

which is the same expression we found in Chapter 2.

3.6 Second Order Tune Shifts

We now use Lie algebra techniques to calculate the second-order tune shifts. These are especially important for sextupoles and decapoles where the first-order tune shifts are zero.

The contributions to f from the normal sextupoles can be written

$$f_s = \sum_i \alpha_i A_{2i} + \frac{1}{2}\sum_{i<j} \alpha_i \alpha_j [A_{2i}, A_{2j}] \quad , \tag{3.42}$$

where α_i is the strength of the i^{th} sextupole (multiplied by the appropriate constants) and A_{2i} is the polynomial

$$\begin{aligned} A_{2i} &= \frac{1}{3}x_i^3 - x_i y_i^2 \\ x_i &= \overline{M}_i x = \sqrt{2\beta_{xi} J_i}\cos(\theta_x + \phi_{xi}) + \eta_{xi}\delta \quad . \end{aligned} \tag{3.43}$$

We will calculate the tune shift for $\delta = 0$. Then we may write

$$x_i = \sqrt{\frac{\beta_{xi} J_x}{2}}\left[e^{i(\theta_x + \phi_{xi})} + cc\right] = \sqrt{\frac{\beta_{xi} J_x}{2}} R_i (e^{i\theta_x} + cc) \tag{3.44}$$

and x_i^n may be written as

$$x_i^n = \left(\frac{\beta_{xi} J_x}{2}\right)^{n/2} R_i (e^{i\theta_x} + cc)^n \quad . \tag{3.45}$$

We are using the notation that

$$R_i f(\theta_x, \theta_y) = f(\theta_x + \phi_{xi}, \theta_y + \phi_{yi}) \tag{3.46}$$

for sextupoles, since $h_{1s} = A_{2i} = 0$, $h_{is} = A_{2i}^- = 0$

$$h_s = h_{2s} = \frac{1}{2}\sum_{i<j} \alpha_i \alpha_j [A_{2i}, A_{2j}]^- + \frac{1}{2}\sum_{i,j} \alpha_i \alpha_j \left[A_{2i}, \frac{1}{1-R} A_{2j}\right]^- \quad . \tag{3.47}$$

This expression involves evaluation for $i \leq j$ of terms of the form

$$G_{ij}^{abcd} = [x_i^a y_i^b, x_j^c y_j^d]^- + \left[x_i^a y_i^b, \frac{1}{1-R} x_j^c y_j^d\right]^- + \left[x_j^a y_j^b, \frac{1}{1-R} x_i^c y_i^d\right]^- \quad . \tag{3.48}$$

One can establish the following facts,

$$
\begin{aligned}
[x_i^a y_i^b, x_j^c y_j^d]^- &= \sum_{\mathbf{n}} g_{ij}^{abcd,\mathbf{n}} \ \sin(\mathbf{n}\cdot\boldsymbol{\phi_{ij}}) \\
[x_i^a y_i^b, \frac{1}{1-R} x_j^c y_j^d]^- &= \sum_{\mathbf{n}} g_{ij}^{abcd,\mathbf{n}} \ \frac{\sin(\mathbf{n}\cdot\boldsymbol{\phi_{ij}}) - \sin[\mathbf{n}\cdot(\boldsymbol{\phi_{ij}}-\boldsymbol{\mu})]}{4\sin^2(\mathbf{n}\cdot\boldsymbol{\mu}/2)}
\end{aligned}
\tag{3.49}
$$

and

$$
G_{ij}^{abcd} = \sum_{\mathbf{n}} g_{ij}^{abcd,\mathbf{n}} \ \frac{\cos[\mathbf{n}\cdot(\boldsymbol{\phi_{ij}}-\boldsymbol{\mu}/\mathbf{2})]}{\sin(\mathbf{n}\cdot\boldsymbol{\mu}/\mathbf{2})} \quad , \tag{3.50}
$$

where

$$
\boldsymbol{\phi_{ij}} = \boldsymbol{\phi_j} - \boldsymbol{\phi_i} \quad . \tag{3.51}
$$

The term for $i = j$ would be obtained by taking the limit $j \to i$ and multiplying by $1/2$. This fact allows us to extend the sum over all i and j where now all terms have a factor of $1/2$. In this sum, we must replace ϕ_{ij} by ϕ_{ij}^+ where

$$
\boldsymbol{\phi_{ij}^+} = \begin{cases} \boldsymbol{\phi_{ij}}, & i < j \\ \boldsymbol{\phi_{ji}}, & j < i \end{cases} \quad . \tag{3.52}
$$

Therefore, we need only find the coefficients of the first simple commutator above to get the $G_{ij}^{abcd,\mathbf{n}}$. The combination of commutators is found by a simple replacement of the sine by another trigonometric function.

Note that only phase differences ϕ_{ij} arise. This follows from

$$
[R_i f, R_j g]^- = [f, R_i^{-1} R_j g]^- = [f, R_{ji} g]^- \quad , \tag{3.53}
$$

where $R_{ji} = R_j R_i^{-1}$. To evaluate the commutators and find the G_{ij}^{abcd}, one can use the basic commutator

$$
[\mathbf{J}^{\mathbf{k}/2} e^{i\mathbf{m}\cdot\boldsymbol{\theta}}, \mathbf{J}^{\mathbf{l}/2} e^{i\mathbf{n}\cdot\boldsymbol{\theta}}] = i \left[\frac{m_x(k_x + l_x)}{2J_x} + \frac{m_y(k_y + l_y)}{2J_y} \right] \delta_{\mathbf{nm}} \mathbf{J}^{(\mathbf{k}+\mathbf{l})/2} \quad , \tag{3.54}
$$

where $\mathbf{J}^{\mathbf{k}} = J_x^{k_x} J_y^{k_y}$.

If we define

$$T_{ij}^{\mathbf{n}} \equiv \frac{\cos[\mathbf{n}\cdot(\boldsymbol{\phi}_{ij}^{+} - \boldsymbol{\mu}/\mathbf{2})]}{\sin(\mathbf{n}\cdot\boldsymbol{\mu}/\mathbf{2})} \quad , \tag{3.55}$$

then the function h_s is given by

$$h_s = \frac{1}{4}\sum_{ij}\alpha_i\alpha_j \sum_{abcd} d_{ab}^{i} d_{cd}^{j} \sum_{n} g_{ij}^{abcd,n} T_{ij}^{\mathbf{n}} \quad , \tag{3.56}$$

where we have written

$$A_{2i} = \sum_{a,b} d_{ab}^{i} x_i^a y_i^b \quad . \tag{3.57}$$

The appropriate coefficients d_{ab}^{i} could be inserted for any multipole.

4. Analytical Expressions for Tune Shift and Smear

The formalism outlined in Chapter 2 gives a recursive formulation for the calculation of tune shift and smear. It proves convenient to implement the recursive formulation in Chapter 2 using a computer algebra system MACSYMA. [15] This allows us to automate the cumbersome analytical forms corresponding to the higher order multipole contributions, as well as to generate the necessary FORTRAN code.

Generally, MACSYMA programs have been written where the input is a definition of the vector potential and the output is analytical expressions for the smear and tune shifts, as well as FORTRAN-compatible expressions. Smear has been calculated to the first order in the multipole strength due to systematic or random a_2 , b_2 , a_3 , b_3 and random a_4 and b_4. For random multipoles, the variance has also been calculated. Tune shifts have been calculated to the second order due to systematic a_2 , b_2 , a_3, and b_3.

4.1 Smear to the First Order in the Multipole Strength

If we define

$$B_{jk}^{n_x n_y} \equiv \frac{\cos(\mathbf{n}\cdot\phi_{jk})}{\sin^2(\pi\mathbf{n}\cdot\nu)} \tag{4.1}$$

and

$$A_j^{m_x m_y} \equiv (2\beta_{xj}J_x)^{m_x/2}(2\beta_{yj}J_y)^{m_y/2} \quad , \tag{4.2}$$

we find

$$\begin{aligned}
S_x^2 = \frac{1}{(2\bar{J}_x)^2}\sum_j\sum_k\Bigg\{ & \frac{1}{32}a_{2j}a_{2k}A_j^{21}A_k^{21}(B_{jk}^{21}+B_{jk}^{2-1}) \\
& + \frac{1}{128}b_{2j}b_{2k}[(4A_j^{12}A_k^{12}-4A_j^{30}A_k^{12}+A_j^{30}A_k^{30})B_{jk}^{10}+A_j^{12}A_k^{12} \\
& \times(B_{jk}^{12}+B_{jk}^{1-2})+A_j^{30}A_k^{30}B_{jk}^{30}] \\
& + \frac{1}{512}a_{3j}a_{3k}[A_j^{13}A_k^{13}(B_{jk}^{13}+B_{jk}^{1-3}+9B_{jk}^{11}+9B_{jk}^{1-1})+9A_j^{31}A_k^{31} \\
& \times(B_{jk}^{31}+B_{jk}^{3-1}+B_{jk}^{11}+B_{jk}^{1-1})-18A_j^{13}A_k^{31}(B_{jk}^{11}+B_{jk}^{1-1})] \\
& + \frac{1}{512}b_{3j}b_{3k}[4(9A_j^{22}A_k^{22}-6A_j^{40}A_k^{22}+A_j^{40}A_k^{40})B_{jk}^{20}+9A_j^{22}A_k^{22} \\
& \times(B_{jk}^{22}+B_{jk}^{2-2})+A_j^{40}A_k^{40}B_{jk}^{40}]\Bigg\}
\end{aligned}$$

$$\begin{aligned}
S_y^2 = \frac{1}{(2\bar{J}_y)^2}\sum_j\sum_k\Bigg\{ & \frac{1}{128}a_{2j}a_{2k}[(4A_j^{21}A_k^{21}-4A_j^{03}A_k^{21}+A_j^{03}A_k^{03})B_{jk}^{01} \\
& + A_j^{21}A_k^{21}(B_{jk}^{21}+B_{jk}^{2-1})+A_j^{03}A_k^{03}B_{jk}^{03}] \\
& + \frac{1}{32}b_{2j}b_{2k}A_j^{12}A_k^{12}(B_{jk}^{12}+B_{jk}^{1-2}) \\
& + \frac{1}{512}a_{3j}a_{3k}[9A_j^{13}A_k^{13}(B_{jk}^{13}+B_{jk}^{1-3}+B_{jk}^{11}+B_{jk}^{1-1})+A_j^{31}A_k^{31} \\
& \times(B_{jk}^{31}+B_{jk}^{3-1}+9B_{jk}^{11}+9B_{jk}^{1-1})-18A_j^{13}A_k^{31}(B_{jk}^{11}+B_{jk}^{1-1})] \\
& + \frac{1}{512}b_{3j}b_{3k}[4(9A_j^{22}A_k^{22}-6A_j^{22}A_k^{04}+A_j^{04}A_k^{04})B_{jk}^{02}+9A_j^{22}A_k^{22} \\
& \times(B_{jk}^{22}+B_{jk}^{2-2})+A_j^{04}A_k^{04}B_{jk}^{04}]\Bigg\}
\end{aligned} \tag{4.3}$$

For systematic multipoles, the sums run over one cell; ν in the denominator of Eq. (4.1) is the phase advance per cell divided by 2π. For random multipoles, the rms smear is obtained by averaging over random seeds so that

$$< a_{nj}a_{nk} >_{\text{seeds}} \rightarrow \sigma^2_{a_jn}\delta_{jk}\,, \qquad < b_{nj}b_{nk} >_{\text{seeds}} \rightarrow \sigma^2_{b_jn}\delta_{jk} \quad , \tag{4.4}$$

where $\sigma_{a_n}\,, \sigma_{b_n}$ are the rms values of the multipole strength. The random multipole errors are assumed to be uncorrelated. Each sum runs over the whole lattice and the phase advance for the entire lattice divided by 2π should be used in Eq. (4.1). However, since the beta functions are periodic with the cell, the sums simplify to a sum over one cell multiplied by the number of cells.

4.2 Tune Shifts to the First Order in the Multipole Strength

To the first order, only quadrupole and octupole errors contribute to the tune shifts (if higher order multipoles are neglected). We have

$$\begin{aligned}
\Delta\nu_x &= \frac{1}{2\pi}\sum_j \left[\frac{1}{2}b_{1j}\beta_{xj} + \frac{3}{4}b_{3j}(\beta^2_{xj}J_x - 2\beta_{xj}\beta_{yj}J_y)\right] \\
\Delta\nu_y &= \frac{1}{2\pi}\sum_j \left[-\frac{1}{2}b_{1j}\beta_{yj} - \frac{3}{4}b_{3j}(2\beta_{xj}\beta_{yj}J_x - \beta^2_{yj}J_y)\right]
\end{aligned} \quad , \tag{4.5}$$

where for systematic errors, the sum runs over one cell and should be multiplied by the number of cells.

4.3 Second Order Tune Shifts

We find for the second order tune shifts

$$
\begin{aligned}
\Delta\nu_x = \frac{1}{2\pi}\sum_j\sum_k \Bigg(
&\frac{1}{8}a_{1j}a_{1k}\sqrt{\beta_{xj}\beta_{xk}\beta_{yj}\beta_{yk}}(T_{jk}^{1-1}-T_{jk}^{11})\\
&+\frac{1}{8}a_{2j}a_{2k}[4(-\beta_{xj}\beta_{xk}\sqrt{\beta_{yj}\beta_{yk}}J_x+\beta_{xj}\sqrt{\beta_{yj}}\beta_{yk}^{3/2}J_y)T_{jk}^{01}-\beta_{xj}\beta_{xk}\sqrt{\beta_{yj}\beta_{yk}}\\
&\times(J_x+2J_y)T_{jk}^{21}+\beta_{xj}\beta_{xk}\sqrt{\beta_{yj}\beta_{yk}}(J_x-2J_y)T_{jk}^{2-1}]\\
&+\frac{1}{8}b_{2j}b_{2k}[(-3\beta_{xj}^{3/2}\beta_{xk}^{3/2}J_x+4\sqrt{\beta_{xj}}\beta_{xk}^{3/2}\beta_{yj}J_y)T_{jk}^{10}-\beta_{xj}^{3/2}\beta_{xk}^{3/2}J_xT_{jk}^{30}\\
&+2\sqrt{\beta_{xj}\beta_{xk}}\beta_{yj}\beta_{yk}J_y(T_{jk}^{1-2}-T_{jk}^{12})]\\
&+\frac{1}{32}a_{3j}a_{3k}\Big\{9\sqrt{\beta_{xj}\beta_{xk}}\beta_{yj}^{3/2}\beta_{yk}^{3/2}J_y^2(T_{jk}^{1-3}-T_{jk}^{13})-3\beta_{xj}^{3/2}\beta_{xk}^{3/2}\sqrt{\beta_{yj}\beta_{yk}}\\
&\times(J_x^2+6J_xJ_y)T_{jk}^{31}+3\beta_{xj}^{3/2}\beta_{xk}^{3/2}\sqrt{\beta_{yj}\beta_{yk}}(J_x^2-6J_xJ_y)T_{jk}^{3-1}+[(-27\\
&\times\sqrt{\beta_{xj}\beta_{xk}}\beta_{yj}^{3/2}\beta_{yk}^{3/2}+36\sqrt{\beta_{xj}}\beta_{xk}^{3/2}\beta_{yj}^{3/2}\sqrt{\beta_{yk}})J_y^2+(72\sqrt{\beta_{xj}}\beta_{xk}^{3/2}\beta_{yj}^{3/2}\sqrt{\beta_{yk}}\\
&-54\beta_{xj}^{3/2}\beta_{xk}^{3/2}\sqrt{\beta_{yj}\beta_{yk}})J_xJ_y-27\beta_{xj}^{3/2}\beta_{xk}^{3/2}\sqrt{\beta_{yj}\beta_{yk}}J_x^2]T_{jk}^{11}+[(27\\
&\times\sqrt{\beta_{xj}\beta_{yk}}\beta_{yj}^{3/2}\beta_{yk}^{3/2}+36\sqrt{\beta_{xj}}\beta_{xk}^{3/2}\beta_{yj}^{3/2}\sqrt{\beta_{yk}})J_y^2+(-72\sqrt{\beta_{xj}}\beta_{xk}^{3/2}\beta_{yj}^{3/2}\sqrt{\beta_{yk}}\\
&-54\beta_{xj}^{3/2}\beta_{xk}^{3/2}\sqrt{\beta_{yj}\beta_{yk}})J_xJ_y+27\beta_{xj}^{3/2}\beta_{xk}^{3/2}\sqrt{\beta_{yj}\beta_{yk}}J_x^2]T_{jk}^{1-1}\Big\}\\
&+\frac{1}{32}b_{3j}b_{3k}\Big\{-9\beta_{xj}\beta_{xk}\beta_{yj}\beta_{yk}(2J_xJ_y+J_y^2)T_{jk}^{22}+9\beta_{xj}\beta_{xk}\beta_{yj}\beta_{yk}(2J_xJ_y\\
&-J_y^2)T_{jk}^{2-2}-3\beta_{xj}^2\beta_{xk}^2J_x^2T_{jk}^{40}+36\beta_{xj}\beta_{yj}\beta_{yk}^2J_y^2T_{jk}^{02}-36\beta_{xj}\beta_{xk}\beta_{yj}\beta_{yk}J_y^2T_{jk}^{20}\\
&+72\beta_{xj}\beta_{xk}^2\beta_{yj}J_xJ_yT_{jk}^{20}-72\beta_{xj}\beta_{xk}\beta_{yj}\beta_{yk}J_xJ_yT_{jk}^{02}-24\beta_{xj}^2\beta_{xk}^2J_x^2T_{jk}^{20}\Big\}\Bigg)
\end{aligned}
$$

$$
\begin{aligned}
\Delta\nu_y = \frac{1}{2\pi}\sum_j\sum_k\Bigg(&-\frac{1}{8}a_{1j}a_{1k}\sqrt{\beta_{xj}\beta_{xk}\beta_{yj}\beta_{yk}}(T_{jk}^{1-1}+T_{jk}^{11})\\
&+\frac{1}{8}a_{2j}a_{2k}[(4\beta_{xj}\sqrt{\beta_{yj}}\beta_{yk}^{3/2}J_x-3\beta_{yj}^{3/2}\beta_{yk}^{3/2}J_y)T_{jk}^{01}+2\beta_{xj}\beta_{xk}\sqrt{\beta_{yj}\beta_{yk}}J_x\\
&\times(T_{jk}^{2-1}-T_{jk}^{21})-\beta_{yj}^{3/2}\beta_{yk}^{3/2}J_yT_{jk}^{03}]\\
&+\frac{1}{8}b_{2j}b_{2k}[4(\sqrt{\beta_{xj}}\beta_{xk}^{3/2}\beta_{yj}J_x-\sqrt{\beta_{xj}\beta_{xk}}\beta_{yj}\beta_{yk}J_y)T_{jk}^{10}-\sqrt{\beta_{xj}\beta_{xk}}\beta_{yj}\beta_{yk}\\
&\times(2J_x+J_y)T_{jk}^{12}-\sqrt{\beta_{xj}\beta_{xk}}\beta_{yj}\beta_{yk}(2J_x-J_y)T_{jk}^{1-2}]\\
&+\frac{1}{32}a_{3j}a_{3k}\Big\{-9\beta_{xj}^{3/2}\beta_{xk}^{3/2}\sqrt{\beta_{yj}\beta_{yk}}J_x^2(T_{jk}^{3-1}+T_{jk}^{31})+3\sqrt{\beta_{xj}\beta_{xk}}\beta_{yj}^{3/2}\beta_{yk}^{3/2}\\
&\times(6J_xJ_y-J_y^2)T_{jk}^{1-3}-3\sqrt{\beta_{xj}\beta_{xk}}\beta_{yj}^{3/2}\beta_{yk}^{3/2}(6J_xJ_y+J_y^2)T_{jk}^{13}+[-27\\
&\times\sqrt{\beta_{xk}\beta_{xk}}\beta_{yj}^{3/2}\beta_{yk}^{3/2}J_y^2+(-54\sqrt{\beta_{xj}\beta_{xk}}\beta_{yk}^{3/2}\beta_{yk}^{3/2}+72\sqrt{\beta_{xj}}\beta_{xk}^{3/2}\beta_{yj}^{3/2}\\
&\times\sqrt{\beta_{yk}})J_xJ_y+(-27\beta_{xj}^{3/2}\beta_{xk}^{3/2}\sqrt{\beta_{yj}\beta_{yk}}+36\sqrt{\beta_{xj}}\beta_{xk}^{3/2}\beta_{yj}^{3/2}\sqrt{\beta_{yk}})J_x^2]T_{jk}^{11}\\
&+[-27\sqrt{\beta_{xj}\beta_{xk}}\beta_{yj}^{3/2}\beta_{yk}^{3/2}J_y^2+(54\sqrt{\beta_{xj}\beta_{xk}}\beta_{yj}^{3/2}\beta_{yk}^{3/2}+72\sqrt{\beta_{xj}}\beta_{xk}^{3/2}\beta_{yj}^{3/2}\\
&\times\sqrt{\beta_{yk}})J_xJ_y+(-27\beta_{xj}^{3/2}\beta_{xk}^{3/2}\sqrt{\beta_{yj}\beta_{yk}}-36\sqrt{\beta_{xj}}\beta_{xk}^{3/2}\beta_{yj}^{3/2}\sqrt{\beta_{yk}})J_x^2]T_{jk}^{1-1}\Big\}\\
&+\frac{1}{32}b_{3j}b_{3k}\Big\{-9\beta_{xj}\beta_{xk}\beta_{yj}\beta_{yk}(2J_xJ_y+J_x^2)T_{jk}^{22}-9\beta_{xj}\beta_{xk}\beta_{yj}\beta_{yk}(2J_xJ_y-J_x^2)\\
&\times T_{jk}^{2-2}-3\beta_{xj}^2\beta_{xk}^2J_y^2T_{jk}^{04}-24\beta_{yj}^2\beta_{yk}^2J_y^2T_{jk}^{02}+72\beta_{xj}\beta_{yj}\beta_{yk}^2J_xJ_yT_{jk}^{02}\\
&-72\beta_{xj}\beta_{xk}\beta_{yj}\beta_{yk}J_xJ_yT_{jk}^{20}+36\beta_{xj}\beta_{xk}^2\beta_{yj}J_x^2T_{jk}^{20}-36\beta_{xj}\beta_{xk}\beta_{yj}\beta_{yk}J_x^2T_{jk}^{02}\Big\}\Bigg)\quad,
\end{aligned}
\tag{4.6}
$$

where $T_{jk}^{n_xn_y}$ is defined by Eq. (3.55).

For systematic errors, each sum runs over one cell and should be multiplied by the number of cells. In Eq. (3.55), the phase advance for one cell divided by 2π should be used for ν.

5. Closed Orbit Perturbations

By realizing that a reasonable correction scheme for closed orbit distortions should lead to local corrections, we conclude that the final corrected orbit can be calculated locally. This can then be done by using the well-known matrix formalism. [7]

5.1 Calculation of the Closed Orbit Distortions

We will assume that a lattice cell for SSC has one horizontal dipole corrector and beam positron monitor (bpm) at each horizontally focusing quadrupole and vice versa for the vertical plane. The ultimate result of the correction scheme is to make the corrected orbit pass through the center of the bpm's. Since there are also bpm errors, this orbit will normally differ from the design orbit.

The calculations will be split in two parts. First, we assume the bpm errors to be zero and calculate the orbit due to dipole errors and quadrupole displacements. The contributions from higher multipoles will be neglected. In the second part, we assume the multipole errors to be zero and calculate the orbit due to the bpm errors. This split can be done since the bpm errors are assumed to be uncorrelated with the multipole errors.

The transfer matrix between two arbitrary points s_0 and s_1 along a lattice

$$\begin{pmatrix} x_1 \\ x_1' \end{pmatrix} = M \begin{pmatrix} x_0 \\ x_0' \end{pmatrix} \quad , \tag{5.1}$$

where

$$M = \begin{pmatrix} \sqrt{\frac{\beta_{x1}}{\beta_{x0}}}[\cos(\Delta\phi_{x10}) + \alpha_{x0}\sin(\Delta\phi_{x10})] & \sqrt{\beta_{x0}\beta_{x1}}\sin(\Delta\phi_{x10}) \\ -\frac{1}{\sqrt{\beta_{x0}\beta_{x1}}}[(1-\alpha_{x0}\alpha_{x1})\sin(\Delta\phi_{x10}) + (\alpha_{x1}-\alpha_{x0})\cos(\Delta\phi_{x10})] & \sqrt{\frac{\beta_{x0}}{\beta_{x1}}}[\cos(\Delta\phi_{x10}) - \alpha_{x1}\sin(\Delta\phi_{x10})] \end{pmatrix} \tag{5.2}$$

and

$$\phi_{x10} \equiv \phi_{x1} - \phi_{x0} \quad . \tag{5.3}$$

If there are no bpm errors, the effect of the correctors is to make the orbit distortions zero at the bpm's (which were assumed to be at the correctors) so that

$$\Delta x_n = \Delta x_0 = 0 \quad . \tag{5.4}$$

If we use the thin lens approximation for the errors and the correctors, we find from Eqs. (5.2) and (5.4)

$$\Delta x_n = \sqrt{\beta_{xn}\beta_{x0}}\sin(\mu_x^{cell})\cdot\Delta x_0' + \sum_{l=1}^{n-1}\sqrt{\beta_{xn}\beta_{xl}}\sin(\Delta\phi_{xnl})\cdot\Delta x_l' = 0 \tag{5.5}$$

or

$$\Delta x_0' = -\sum_{l=1}^{n-1}\sqrt{\frac{\beta_{xl}}{\beta_{x0}}}\frac{\sin(\Delta\phi_{xnl})}{\sin(\mu_x^{cell})}\Delta x_l' \quad , \tag{5.6}$$

where

$$\Delta x_l' = -\theta_d(b_0 + b_1\Delta x_{\rm quad}) \tag{5.7}$$

and $\Delta x_{\rm quad}$ is the quadrupole misalignment, since higher order multipoles are neglected. By using

$$\Delta x_j = \sum_{l=0}^{<j}\sqrt{\beta_{xj}\beta_{xl}}\sin(\Delta\phi_{xjl})\cdot\Delta x_l' \,, \qquad 0 \le j \le n \quad , \tag{5.8}$$

we find

$$\begin{aligned}\Delta x_j = &-\sum_{l=1}^{<j}\sqrt{\beta_{xj}\beta_{xl}}\sin(\Delta\phi_{xj0})\cdot\frac{\sin(\Delta\phi_{xnl})}{\sin(\mu_x^{cell})}\cdot\Delta x_l' \\ &+\sum_{l=1}^{<j}\sqrt{\beta_{xj}\beta_{xl}}\sin(\Delta\phi_{xjl})\cdot x_l' \quad .\end{aligned} \tag{5.9}$$

By using some trigonometric relations, this can be written

$$\Delta x_j^{\rm mp} = -\frac{1}{\sin(\mu_x^{cell})}\left[\sum_{l=1}^{<j}\sqrt{\beta_{xj}\beta_{xl}}\Delta x_l' \sin(\Delta\phi_{xnj})\sin(\Delta\phi_{xl0}) + \sum_{l=j}^{n-1}\sqrt{\beta_{xj}\beta_{xl}}\Delta x_l' \sin(\Delta\phi_{xj0})\sin(\Delta\phi_{xnl})\right], \qquad 0 \le j \le n \quad . \tag{5.10}$$

We now assume the multipole errors to be zero and that the correctors have been adjusted so that the new orbit passes through the centers of the bpm's. From Eq. (5.2), we have

$$\Delta x_n = \sqrt{\frac{\beta_{xn}}{\beta_{x0}}}[\cos(\Delta\phi_{xn0}) + \alpha_{x0}\sin(\Delta\phi_{xn0})]\Delta x_0 + \sqrt{\beta_{xn}\beta_{x0}}\sin(\Delta\phi_{xn0})\cdot\Delta x_0' \quad . \tag{5.11}$$

The β-function is periodic, hence

$$\beta_{xn} = \beta_{x0} \tag{5.12}$$

so that

$$\Delta x_0' = \frac{1}{\beta_{x0}\sin(\mu_x^{cell})}\{\Delta x_n - [\cos(\mu_x^{cell}) + \alpha_x^0\sin(\mu_x^{cell})\Delta x_0]\}] \quad . \tag{5.13}$$

In a similar way, we obtain

$$\Delta x_j^{\rm bpm} = \frac{1}{\sin(\mu_x^{cell})}\sqrt{\frac{\beta_{xj}}{\beta_{x0}}}[\sin(\Delta\phi_{xnj})\cdot\Delta x_0 + \sin(\Delta\phi_{xj0})\cdot\Delta x_n] \quad . \tag{5.14}$$

Since we assume the multipole misalignment and bpm displacement errors to be uncorrelated, we finally obtain

$$\Delta x_j^{\rm co} = \sqrt{(\Delta x_j^{\rm mp})^2 + (\Delta x_j^{\rm bpm})^2} \quad . \tag{5.15}$$

5.2 Calculation of the Feed-down

The feed-down is calculated by generalizing Eq. (2.23) to

$$V = \theta_d Re \sum_{n=0}^{\infty} \frac{1}{n+1}(b_n + ia_n)\,[x + \Delta x + i(y + \Delta y)]^{n+1} \quad , \tag{5.16}$$

where Δx and Δy is the horizontal and vertical orbit. If we restrict ourselves to terms linear in Δx or Δy, we find the following contributions from the feed-down

$$\begin{aligned} a_{n-1} &= n(a_n \Delta x + b_n \Delta y) + O(2) \\ b_{n-1} &= -n(a_n \Delta y - b_n \Delta x) + O(2) \quad . \end{aligned} \tag{5.17}$$

This approximation is expected to be good as long as $\Delta x \ll A_x$ and $\Delta y \ll A_y$. When these terms are inserted in the equations for S^2, Eqs. (4.3), and we average over random seeds, we find

$$\begin{aligned} b_{nj} b_{nk} \sim\ & a_{(n+1),j} a_{(n+1),k} < \Delta y_j \Delta y_k >_{\text{seeds}} \\ & + b_{(n+1),j} b_{(n+1),k} < \Delta x_j \Delta x_k >_{\text{seeds}} + O(2) \end{aligned} \tag{5.18}$$

for systematic multipoles and

$$< b_{nj} b_{nk} >_{\text{seeds}} \sim [\sigma^2_{a_{(n+1),j}} < \Delta y_j^2 >_{\text{seeds}} + \sigma^2_{b_{(n+1),j}} < \Delta x_j^2 >_{\text{seeds}}] \delta_{jk} + O(2) \tag{5.19}$$

for random multipoles, since $\Delta x\,, \Delta y$ and the multipole errors are assumed to be uncorrelated. The correlations $< \Delta x_j \Delta x_k >_{\text{seeds}}$ and $< \Delta y_j \Delta y_k >_{\text{seeds}}$ are calculated from Eq. (5.16).

6. Chromatic Perturbations

The chromatic perturbations can be treated as a feed-down where the orbit is given by the nonlinear dispersion function η

$$\Delta x = \delta\eta = \delta(\eta_0 + \delta\eta_1 + ...) \quad , \tag{6.1}$$

where η_0 is the linear dispersion function. Furthermore, the multipole strength is replaced by an effective multipole strength given by

$$b_n = \frac{1}{1+\delta} b_n = (1 - \delta + \delta^2 - ...) b_n \quad . \tag{6.2}$$

Since the linear chromaticity is corrected, one would like to calculate the chromaticity to at least quadratic terms in δ. From above, it is, however, clear that this requires a knowledge of η_1. It can be calculated,[16] but a direct numerical calculation of the tune shift using map techniques would be more efficient.[17] The previous work has, therefore, been limited to the on-momentum case.

7. Numerical Results

In the expressions for the smear, Eqs. (4.3), we find terms proportional to

$$\frac{1}{\sin^2(\pi\nu)} \qquad \frac{1}{\sin^2(\pi 2\nu)} \tag{7.1}$$

from sextupoles and the octupoles. The first case may be interpreted as orbit terms and the second will only change the average amplitude. Since the perturbations of these terms is similar to dipole and quadrupole perturbations (but amplitude dependent) and to simplify the analysis of the tracking data, they have been excluded in the following calculations.

We have studied FODO-lattices with identical approximately 90 degree cells for an injection energy of 1 or 2 TeV, 4 or 5 cm magnet aperture and injection optics.

Table 1: Studied cases.

No. of dipoles per half cell	Half cell length	No. of cells	ν_x	ν_y	$A_x = A_y$ (mm) 1TeV	2TeV	$\delta\,(10^{-3})$ 1TeV	2TeV
4	84.20	480	121.285	122.265	4.15	3.73	0	0
					2.75	2.33	1.36	0.68
5	98.62	384	97.285	98.265	4.43	3.97	0	0
					2.92	2.46	1.16	0.58
6	114.25	320	81.285	82.265	4.73	4.18	0	0
					3.10	2.55	1.0	0.50

Table 2: Multipole errors in the dipoles.

	Random errors		Systematic errors			
Multipole	4cm	5cm	1TeV, 4cm	1TeV, 5cm	2Tev, 4cm	2TeV, 5cm
a_0	6.0	6.0	0	0	0	0
b_0	6.0	6.0	0	0	0	0
a_1	0.7	0.56	0.2	0.2	0.15	0.15
b_1	0.7	0.56	0.2	0.2	0.15	0.15
a_2	0.6	0.41	0.1	0.1	0.06	0.06
b_2	0.4	0.27	-8.4	-4.0	-5.33	-2.53
a_3	0.7	0.41	0.2	0.2	0.11	0.11
b_3	0.3	0.18	0.1	0.1	0.05	0.05
a_4	0.2	0.10	0.2	0.2	0.09	0.09
b_4	0.7	0.35	0.84	0.5	0.39	0.18

The total number of dipoles has been kept to 3840, but the number of dipoles per cell and the number of cells have been varied. The cases that have been

studied are shown in Table 1. [11, 18] Closed orbit distortions have been calculated for

$$\Delta x_{\rm quad}^{\rm rms} = 1.00 \text{ mm}, \qquad \Delta x_{\rm bpm}^{\rm rms} = 1.41 \text{ mm} \tag{7.2}$$

with respect to the design orbit. The linear aperture may be defined by 6.4% smear [4] and a tune shift of 5×10^{-3}. [1] The linear lattice functions were calculated by TEAPOT. [19] After the systematic multipole errors had been added, the linear chromaticity was tuned to zero using TEAPOT. The strength obtained for the chromaticity sextupoles were then used in the analytical calculations. Calculations have also been done with the "SNEUFF" correction scheme. [1] In this case, the chromaticity was tuned after the the correctors had been added. Correctors were added for a_2 , b_2 , a_3, and b_3.

7.1 Smear and Tune Shifts

In Tables 3 to 15, we present the smear and tune shifts for the different cases specified in Table 1. For random multipoles, we give the average smear and the spread of the total smear as defined by Eqs. (2.2) and (2.3). An empty location indicates that no value has been calculated. Linear coupling perturbations due to feed-down in the sextupoles are presented (in the column (a_1)), but are not included in the total. The total tune shifts are obtained by summing up the individual terms, whereas for the total smear one has to sum the square of the different contributions and then take the square root. Note that if the linear lattice functions are given, the results in one of the tables displayed below, is obtained in less than a minute on the VAX.

Table 3 shows a case when the horizontal and vertical tune have not been splitted by one unit ($\nu_x = 81.285$, $\nu_y = 81.265$). As expected, this leads to very high contributions from the systematic errors.

Table 3a: 6 dipoles, 1 TeV, 4 cm magnet aperture, no split.

Smear (%)	(a_1)	a_2	b_2	a_3	b_3	a_4	b_4	Total
Due to random multipoles		1.4	0.8	2.3	0.5	0.1	0.2	2.9±0.8
		1.0	0.9	2.4	0.6	0.0	0.2	2.8±0.6
Due to feed-down in the	6.2	0.6	0.4	1.0	0.5			1.3
random multipoles	6.2	0.4	0.6	1.1	0.5			1.4
Due to systematic multipoles		0.0	1.0	0.1	8.0			8.1
		0.0	0.5	0.1	8.0			8.0
Due to feed-down in the	>100	0.0	0.0	17.0	24.3			29.7
systematic multipoles	>100	0.0	0.0	17.0	24.3			29.7
Due to corrected		0.0	0.5	0.6	0.1			0.8
systematic multipoles		0.0	0.3	0.6	0.1			0.7
Due to feed-down in the	>100	0.0	0.0	0.0	4.8			4.8
corr. systematic multipoles	>100	0.0	0.0	0.0	4.8			4.8
$\Delta\nu\,(10^{-3})$	a_2^2	b_2^2	b_3	a_3^2	b_3^2			Total
Due to systematic multipoles	0.0	22.5	-2.4	-29.9	0.6			-9.2
	0.0	31.1	-2.4	29.8	-0.6			57.9
Due to corrected	0.0	6.4	0.2	0.0	0.0			6.5
systematic multipoles	0.0	6.1	0.2	0.0	0.0			6.3

Table 3b: 6 dipoles, 1 TeV, 4 cm magnet aperture.

Smear (%)	(a_1)	a_2	b_2	a_3	b_3	a_4	b_4	Total
Due to random multipoles		1.4	0.8	2.5	0.5	0.1	0.2	3.0±1.4
		1.0	0.9	2.5	0.6	0.0	0.2	2.9±1.3
Due to feed-down in the	6.7	0.6	0.4	1.1	0.5			1.4
random multipoles	6.6	0.4	0.6	1.1	0.5			1.4
Due to systematic multipoles		0.0	1.0	0.1	0.2			1.1
		0.0	0.5	0.1	0.2			0.5
Due to feed-down in the	27.6	0.0	0.0	0.4	0.6			0.7
systematic multipoles	27.6	0.0	0.0	0.4	0.6			0.7
Due to corrected		0.0	0.5	0.0	0.0			0.5
systematic multipoles		0.0	0.3	0.0	0.0			0.3
Due to feed-down in the	11.6	0.0	0.0	0.0	0.1			0.1
corr. systematic multipoles	11.5	0.0	0.0	0.0	0.1			0.1
$\Delta\nu\,(10^{-3})$	a_2^2	b_2^2	b_3	a_3^2	b_3^2			Total
Due to systematic multipoles	0.0	22.7	-2.3	0.7	0.0			21.0
	0.0	31.5	-2.4	-0.7	0.0			28.4
Due to corrected	0.0	6.3	0.2	0.0	0.0			6.5
systematic multipoles	0.0	6.0	0.2	0.0	0.0			6.1

Table 4: 6 dipoles, 2 TeV, 4 cm magnet aperture.

Smear (%)	(a_1)	a_2	b_2	a_3	b_3	a_4	b_4	Total
Due to random multipoles		1.2	0.7	1.9	0.4	0.0	0.1	2.5±1.1
		0.9	0.8	2.0	0.4	0.0	0.1	2.4±1.0
Due to feed-down in the	6.7	0.5	0.4	0.8	0.4			1.1
random multipoles	6.6	0.3	0.5	0.9	0.4			1.1
Due to systematic multipoles		0.0	0.5	0.1	0.1			0.5
		0.0	0.2	0.0	0.1			0.3
Due to feed-down in the	13.8	0.0	0.0	0.2	0.3			0.3
systematic multipoles	13.8	0.0	0.0	0.2	0.3			0.3
Due to corrected		0.0	0.2	0.0	0.0			0.2
systematic multipoles		0.0	0.2	0.0	0.0			0.2
Due to feed-down in the	5.9	0.0	0.0	0.0	0.1			0.1
corr. systematic multipoles	5.9	0.0	0.0	0.0	0.1			0.1
$\Delta\nu\,(10^{-3})$	a_2^2	b_2^2	b_3	a_3^2	b_3^2			Total
Due to systematic multipoles	0.0	3.9	-1.8	0.4	0.0			2.5
	0.0	4.5	-1.9	-0.4	0.0			2.2
Due to corrected	0.0	1.1	0.1	0.0	0.0			1.2
systematic multipoles	0.0	1.0	0.1	0.0	0.0			1.1

Table 5: 6 dipoles, 1 TeV, 5 cm magnet aperture.

Smear (%)	(a_1)	a_2	b_2	a_3	b_3	a_4	b_4	Total
Due to random multipoles		1.0	0.6	1.5	0.3	0.0	0.1	1.9±0.8
		0.7	0.6	1.5	0.3	0.0	0.1	1.8±0.8
Due to feed-down in the	4.5	0.3	0.3	0.5	0.3			0.7
random multipoles	4.5	0.2	0.3	0.6	0.3			0.7
Due to systematic multipoles		0.0	0.7	0.0	0.1			0.7
		0.0	0.3	0.0	0.1			0.4
Due to feed-down in the	18.0	0.0	0.0	0.2	0.3			0.3
systematic multipoles	17.9	0.0	0.0	0.2	0.3			0.3
Due to corrected		0.0	0.3	0.0	0.0			0.3
systematic multipoles		0.0	0.2	0.0	0.0			0.2
Due to feed-down in the	7.5	0.0	0.0	0.0	0.1			0.1
corr. systematic multipoles	7.5	0.0	0.0	0.0	0.1			0.1
$\Delta\nu\,(10^{-3})$	a_2^2	b_2^2	b_3	a_3^2	b_3^2			Total
Due to systematic multipoles	0.0	9.0	-1.2	0.2	0.0			8.1
	0.0	11.4	-1.2	-0.2	0.0			10.0
Due to corrected	0.0	2.5	0.1	0.0	0.0			2.6
systematic multipoles	0.0	2.3	0.1	0.0	0.0			2.4

Table 6: 6 dipoles, 2 TeV, 5 cm magnet aperture.

Smear (%)	(a_1)	a_2	b_2	a_3	b_3	a_4	b_4	Total
Due to random multipoles		0.8	0.5	1.1	0.2	0.0	0.1	1.5±0.7
		0.6	0.5	1.2	0.3	0.0	0.1	1.4±0.6
Due to feed-down in the	4.5	0.3	0.2	0.4	0.2			0.6
random multipoles	4.5	0.2	0.3	0.4	0.2			0.6
Due to systematic multipoles		0.0	0.3	0.0	0.1			0.3
		0.0	0.2	0.0	0.1			0.2
Due to feed-down in the	9.3	0.0	0.0	0.1	0.1			0.1
systematic multipoles	9.2	0.0	0.0	0.1	0.1			0.1
Due to corrected		0.0	0.2	0.0	0.0			0.2
systematic multipoles		0.0	0.1	0.0	0.0			0.1
Due to feed-down in the	4.2	0.0	0.0	0.0	0.0			0.0
corr. systematic multipoles	4.2	0.0	0.0	0.0	0.0			0.0
$\Delta\nu\,(10^{-3})$		a_2^2	b_2^2	b_3	a_3^2	b_3^2		Total
Due to systematic multipoles	0.0	1.5	-0.9	0.0	0.0			0.6
	0.0	1.3	-0.9	0.0	0.0			0.3
Due to corrected	0.0	0.4	0.1	0.0	0.0			0.5
systematic multipoles	0.0	0.4	0.1	0.0	0.0			0.4

Table 7: 5 dipoles, 1 TeV, 4 cm magnet aperture.

Smear (%)	(a_1)	a_2	b_2	a_3	b_3	a_4	b_4	Total
Due to random multipoles		1.1	0.7	1.9	0.4	0.0	0.1	2.3±1.0
		0.8	0.7	1.9	0.4	0.0	0.1	2.2±1.0
Due to feed-down in the	5.8	0.5	0.4	0.8	0.4			1.1
random multipoles	5.7	0.3	0.5	0.8	0.4			1.1
Due to systematic multipoles		0.0	0.7	0.1	0.1			0.8
		0.0	0.4	0.0	0.1			0.4
Due to feed-down in the	25.8	0.0	0.0	0.3	0.4			0.5
systematic multipoles	25.7	0.0	0.0	0.3	0.4			0.5
Due to corrected		0.0	0.4	0.0	0.0			0.4
systematic multipoles		0.0	0.2	0.0	0.0			0.2
Due to feed-down in the	10.4	0.0	0.0	0.0	0.1			0.1
corr. systematic multipoles	10.4	0.0	0.0	0.0	0.1			0.1
$\Delta\nu\,(10^{-3})$		a_2^2	b_2^2	b_3	a_3^2	b_3^2		Total
Due to systematic multipoles	0.0	12.3	1.9	0.4	0.0			10.7
	0.0	14.5	-1.9	-0.4	0.0			12.2
Due to corrected	0.0	3.5	0.1	0.0	0.0			3.6
systematic multipoles	0.0	3.3	0.1	0.0	0.0			3.4

Table 8: 5 dipoles, 2 TeV, 4 cm magnet aperture.

Smear (%)	(a_1)	a_2	b_2	a_3	b_3	a_4	b_4	Total
Due to random multipoles		1.0	0.6	1.5	0.3	0.0	0.1	1.9±0.9
		0.7	0.7	1.5	0.3	0.0	0.1	1.9±0.8
Due to feed-down in the	5.8	0.4	0.3	0.7	0.3			0.9
random multipoles	5.7	0.3	0.4	0.7	0.3			0.9
Due to systematic multipoles		0.0	0.4	0.0	0.1			0.4
		0.0	0.2	0.0	0.1			0.2
Due to feed-down in the	13.3	0.0	0.0	0.1	0.2			0.3
systematic multipoles	13.3	0.0	0.0	0.1	0.2			0.3
Due to corrected		0.0	0.2	0.0	0.0			0.2
systematic multipoles		0.0	0.2	0.0	0.0			0.2
Due to feed-down in the	6.0	0.0	0.0	0.0	0.1			0.1
corr. systematic multipoles	6.0	0.0	0.0	0.0	0.0			0.0
$\Delta\nu\,(10^{-3})$	a_2^2	b_2^2	b_3	a_3^2	b_3^2			Total
Due to systematic multipoles	0.0	2.1	-1.5	0.2	0.0			0.8
	0.0	1.4	-1.5	-0.3	0.0			-0.4
Due to corrected	0.0	0.5	0.1	0.0	0.0			0.7
systematic multipoles	0.0	0.5	0.1	0.0	0.0			0.6

Table 9: 5 dipoles, 1 TeV, 5 cm magnet aperture.

Smear (%)	(a_1)	a_2	b_2	a_3	b_3	a_4	b_4	Total
Due to random multipoles		0.8	0.4	1.1	0.2	0.0	0.1	1.4±0.6
		0.6	0.5	1.1	0.3	0.0	0.1	1.4±0.6
Due to feed-down in the	3.9	0.3	0.2	0.4	0.2			0.6
random multipoles	3.9	0.2	0.3	0.4	0.2			0.6
Due to systematic multipoles		0.0	0.5	0.0	0.1			0.5
		0.0	0.3	0.0	0.1			0.3
Due to feed-down in the	17.0	0.0	0.0	0.1	0.2			0.2
systematic multipoles	17.0	0.0	0.0	0.1	0.2			0.2
Due to corrected		0.0	0.3	0.0	0.0			0.3
systematic multipoles		0.0	0.2	0.0	0.0			0.2
Due to feed-down in the	7.3	0.0	0.0	0.0	0.0			0.0
corr. systematic multipoles	7.2	0.0	0.0	0.0	0.0			0.0
$\Delta\nu\,(10^{-3})$	a_2^2	b_2^2	b_3	a_3^2	b_3^2			Total
Due to systematic multipoles	0.0	4.8	-0.9	0.1	0.0			3.9
	0.0	4.5	-1.0	-0.1	0.0			3.4
Due to corrected	0.0	1.3	0.1	0.0	0.0			1.4
systematic multipoles	0.0	1.2	0.1	0.0	0.0			1.3

Table 10: 5 dipoles, 2 TeV, 5 cm magnet aperture.

Smear (%)	(a_1)	a_2	b_2	a_3	b_3	a_4	b_4	Total
Due to random multipoles		0.7	0.4	0.9	0.2	0.0	0.0	1.2±0.5
		0.5	0.4	0.9	0.2	0.0	0.1	1.1±0.5
Due to feed-down in the	3.9	0.2	0.2	0.3	0.2			0.5
random multipoles	3.9	0.2	0.2	0.3	0.2			0.5
Due to systematic multipoles		0.0	0.3	0.0	0.1			0.3
		0.0	0.2	0.0	0.1			0.2
Due to feed-down in the	9.4	0.0	0.0	0.1	0.1			0.1
systematic multipoles	9.4	0.0	0.0	0.1	0.1			0.1
Due to corrected		0.0	0.2	0.0	0.0			0.2
systematic multipoles		0.0	0.2	0.0	0.0			0.2
Due to feed-down in the	3.2	0.0	0.0	0.0	0.0			0.0
corr. systematic multipoles	3.2	0.0	0.0	0.0	0.0			0.0
$\Delta\nu\,(10^{-3})$		a_2^2	b_2^2	b_3	a_3^2	b_3^2		Total
Due to systematic multipoles		0.0	0.7	-0.8	0.0	0.0		0.0
		0.0	0.0	-0.8	0.0	0.0		-0.8
Due to corrected		0.0	-0.3	0.1	0.0	0.0		-0.3
systematic multipoles		0.0	0.2	0.1	0.0	0.0		0.3

Table 11: 4 dipoles, 1 TeV, 4 cm magnet aperture.

Smear (%)	(a_1)	a_2	b_2	a_3	b_3	a_4	b_4	Total
Due to random multipoles		0.9	0.5	1.4	0.3	0.0	0.1	1.8±0.8
		0.6	0.6	1.4	0.3	0.0	0.1	1.7±0.7
Due to feed-down in the	4.9	0.4	0.3	0.6	0.3			0.8
random multipoles	4.9	0.2	0.4	0.6	0.3			0.8
Due to systematic multipoles		0.0	0.5	0.0	0.1			0.5
		0.0	0.3	0.0	0.1			0.3
Due to feed-down in the	24.2	0.0	0.0	0.2	0.3			0.4
systematic multipoles	24.2	0.0	0.0	0.2	0.3			0.4
Due to corrected		0.0	0.3	0.0	0.0			0.3
systematic multipoles		0.0	0.3	0.0	0.0			0.3
Due to feed-down in the	10.6	0.0	0.0	0.0	0.1			0.1
corr. systematic multipoles	10.6	0.0	0.0	0.0	0.1			0.1
$\Delta\nu\,(10^{-3})$		a_2^2	b_2^2	b_3	a_3^2	b_3^2		Total
Due to systematic multipoles		0.0	6.2	-1.6	0.2	0.0		4.9
		0.0	4.3	-1.6	-0.2	0.0		2.5
Due to corrected		0.0	1.8	0.1	0.0	0.0		1.9
systematic multipoles		0.0	1.4	0.1	0.0	0.0		1.6

Table 12: 4 dipoles, 2 TeV, 4 cm magnet aperture.

Smear (%)	(a_1)	a_2	b_2	a_3	b_3	a_4	b_4	Total
Due to random multipoles		0.8	0.5	1.1	0.2	0.0	0.1	1.5±0.6
		0.6	0.5	1.1	0.3	0.0	0.1	1.4±0.6
Due to feed-down in the	4.9	0.3	0.3	0.5	0.2			0.7
random multipoles	4.9	0.2	0.3	0.5	0.3			0.7
Due to systematic multipoles		0.0	0.3	0.0	0.1			0.3
		0.0	0.2	0.0	0.1			0.2
Due to feed-down in the	14.0	0.0	0.0	0.1	0.2			0.2
systematic multipoles	14.0	0.0	0.0	0.1	0.2			0.2
Due to corrected		0.0	0.2	0.0	0.0			0.2
systematic multipoles		0.0	0.2	0.0	0.0			0.2
Due to feed-down in the	8.2	0.0	0.0	0.0	0.0			0.0
corr. systematic multipoles	8.2	0.0	0.0	0.0	0.0			0.0
$\Delta\nu\,(10^{-3})$	a_2^2	b_2^2	b_3	a_3^2	b_3^2			Total
Due to systematic multipoles	0.0	0.8	-1.3	0.1	0.0			-0.3
	0.0	-0.6	-1.3	-0.1	0.0			-2.0
Due to corrected	0.0	0.1	0.1	0.0	0.0			0.2
systematic multipoles	0.0	0.0	0.1	0.0	0.0			0.2

Table 13: 4 dipoles, 1 TeV, 5 cm magnet aperture.

Smear (%)	(a_1)	a_2	b_2	a_3	b_3	a_4	b_4	Total
Due to random multipoles		0.6	0.4	0.8	0.2	0.0	0.0	1.1±0.5
		0.4	0.4	0.8	0.2	0.0	0.1	1.0±0.4
Due to feed-down in the	3.4	0.2	0.2	0.3	0.2			0.4
random multipoles	3.4	0.1	0.2	0.3	0.2			0.4
Due to systematic multipoles		0.0	0.4	0.0	0.1			0.4
		0.0	0.3	0.0	0.1			0.3
Due to feed-down in the	17.0	0.0	0.0	0.1	0.2			0.2
systematic multipoles	16.9	0.0	0.0	0.1	0.2			0.2
Due to corrected		0.0	0.2	0.0	0.0			0.2
systematic multipoles		0.0	0.2	0.0	0.0			0.2
Due to feed-down in the	8.8	0.0	0.0	0.0	0.0			0.0
corr. systematic multipoles	8.8	0.0	0.0	0.0	0.0			0.0
$\Delta\nu\,(10^{-3})$	a_2^2	b_2^2	b_3	a_3^2	b_3^2			Total
Due to systematic multipoles	0.0	2.2	-0.8	0.1	0.0			1.5
	0.0	0.1	-0.8	-0.1	0.0			-0.7
Due to corrected	0.0	0.5	0.1	0.0	0.0			0.6
systematic multipoles	0.0	0.4	0.1	0.0	0.0			0.4

Table 14: 4 dipoles, 2 TeV, 5 cm magnet aperture.

Smear (%)	(a_1)	a_2	b_2	a_3	b_3	a_4	b_4	Total
Due to random multipoles		0.6	0.3	0.7	0.1	0.0	0.0	0.9±0.4
		0.4	0.4	0.7	0.2	0.0	0.0	0.9±0.4
Due to feed-down in the	3.4	0.2	0.2	0.2	0.1			0.4
random multipoles	3.4	0.1	0.2	0.2	0.1			0.4
Due to systematic multipoles		0.0	0.4	0.0	0.0			0.4
		0.0	0.2	0.0	0.0			0.2
Due to feed-down in the	18.4	0.0	0.0	0.0	0.1			0.1
systematic multipoles	18.3	0.0	0.0	0.0	0.1			0.1
Due to corrected		0.0	0.2	0.0	0.0			0.2
systematic multipoles		0.0	0.2	0.0	0.0			0.2
Due to feed-down in the	7.8	0.0	0.0	0.0	0.0			0.0
corr. systematic multipoles	7.8	0.0	0.0	0.0	0.0			0.0
$\Delta\nu\,(10^{-3})$	a_2^2	b_2^2	b_3	a_3^2	b_3^2			Total
Due to systematic multipoles	0.0	0.4	-0.6	0.0	0.0			-0.2
	0.0	2.9	-0.6	0.0	0.0			2.3
Due to corrected	0.0	-0.1	0.1	0.0	0.0			-0.1
systematic multipoles	0.0	-0.1	0.1	0.0	0.0			-0.1

7.2 Smear versus Tune

The analytical expressions for the smear may be used to study the dependence on the working point. Since the main contribution is from the random multipoles, only these will be considered without feed-down. Figure 1 to 6 shows contour plots of $\max(S_x\,, S_y)$ for the cases of 4 cm magnet aperture from Table 1. The contour plots were obtained by calculating smear values for a 100×100 grid and using TOPDRAWER. [20] Since the smear goes to infinity on the resonances, the values above 100% were cut. The wiggling of the contour lines close to the resonances is due to the interpolation between grid points.

It is clear from the plots that if only smear is considered a more favorable working point than the normal

$$\nu_x = 81.285\,, \qquad \nu_y = 82.265 \tag{7.3}$$

would be, e.g.,

$$\nu_x = 81.38\,, \qquad \nu_y = 82.44 \tag{7.4}$$

for the 6 dipoles case.

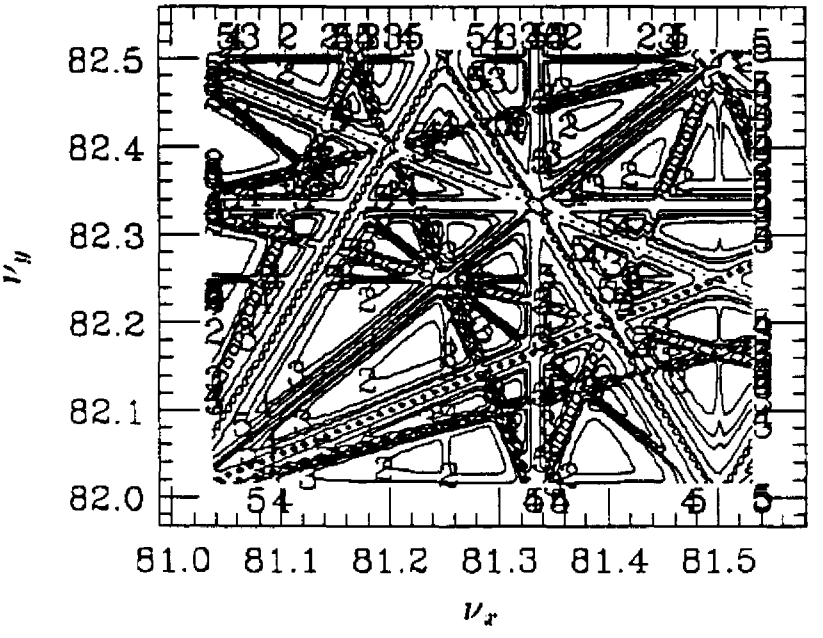

Figure 1: 6 dipoles, 1 TeV, 4 cm

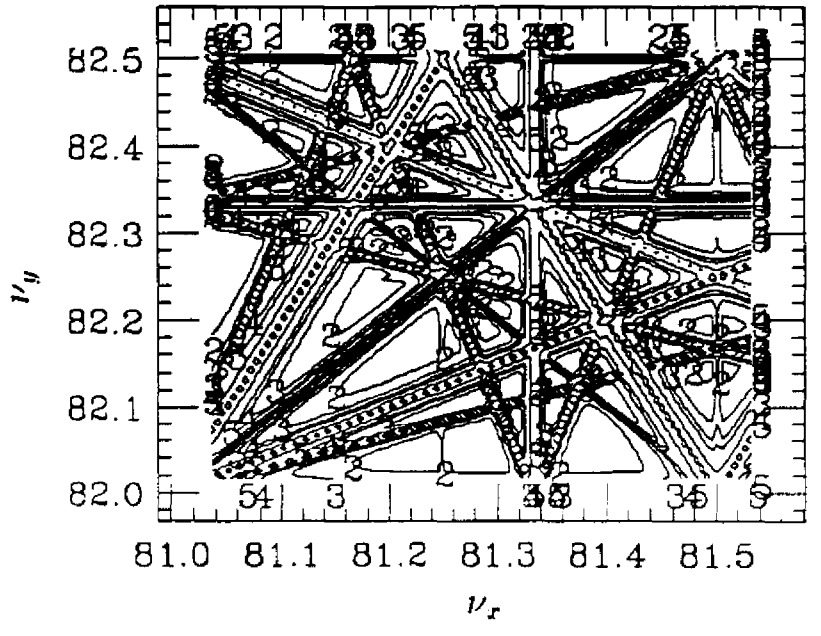

Figure 2: 6 dipoles, 2 TeV, 4 cm

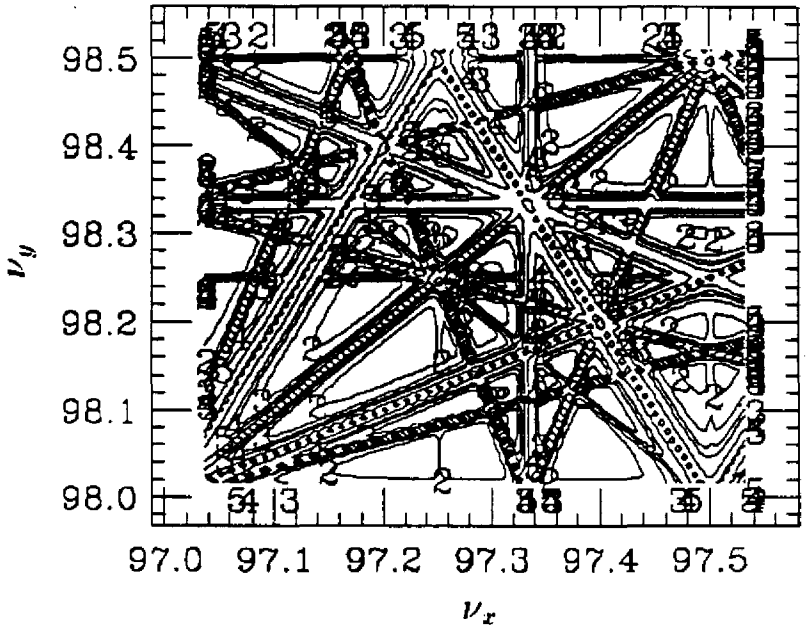

Figure 3: 5 dipoles, 1 TeV, 4 cm

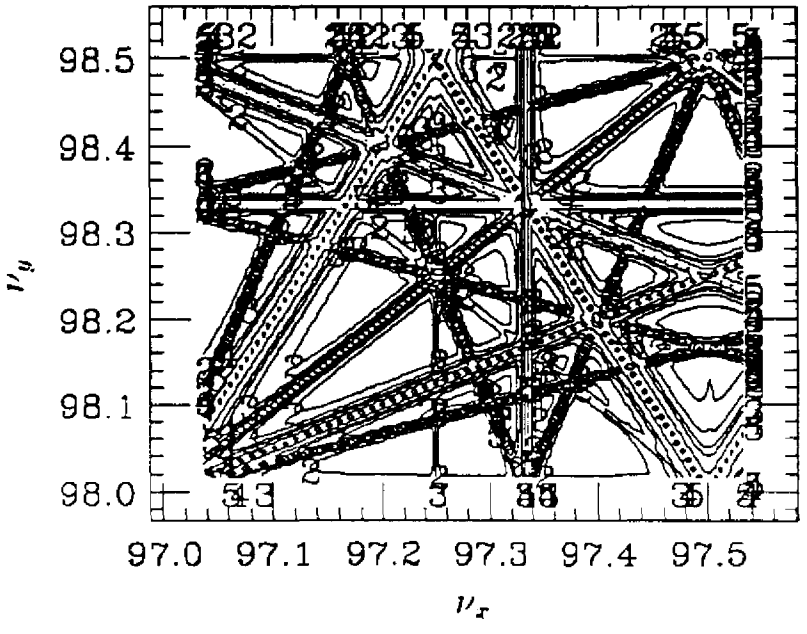

Figure 4: 5 dipoles, 2 TeV, 4 cm

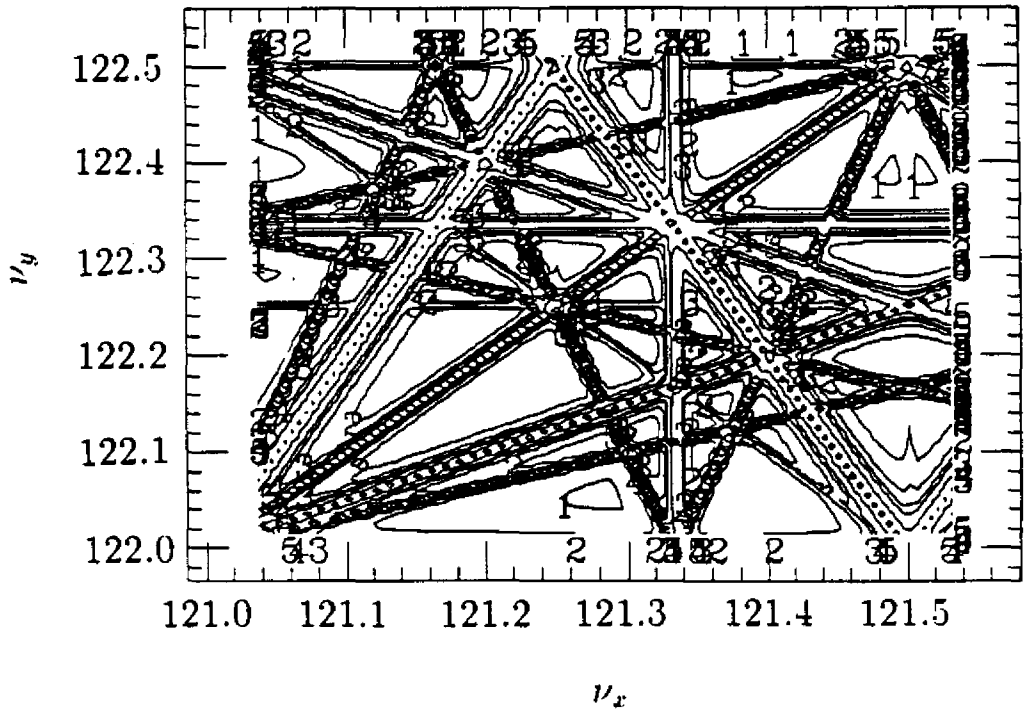

Figure 5: 4 dipoles, 1 TeV, 4 cm

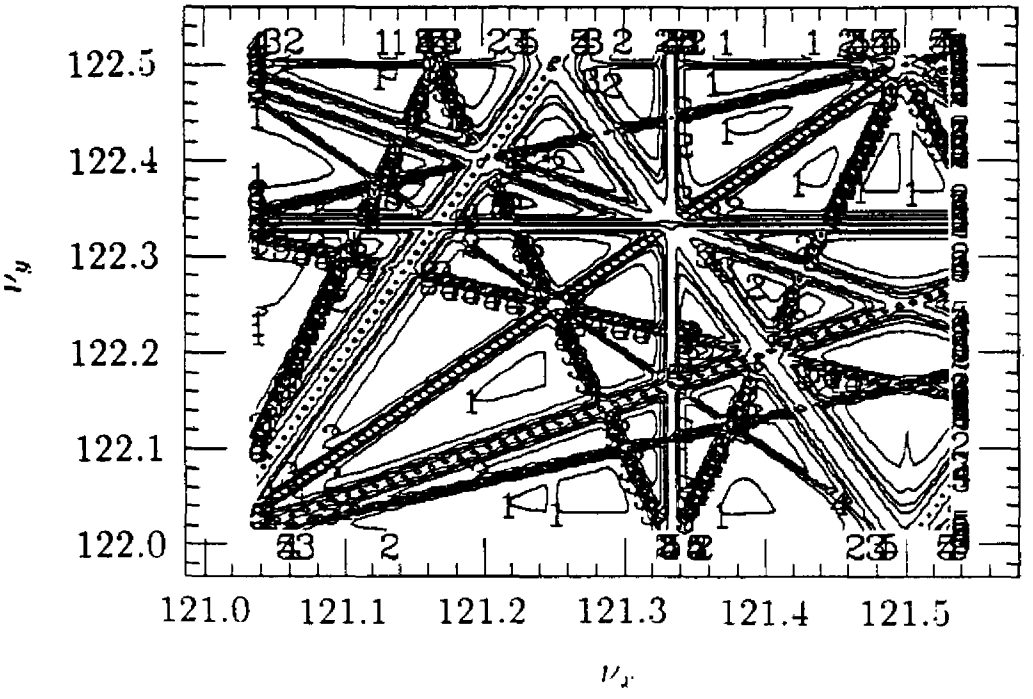

Figure 6: 4 dipoles, 2 TeV, 4 cm

8. Comparison with Tracking

In the following sections, we will quote numbers obtained from numerical simulations followed by numbers within brackets corresponding to analytically calculated values. The results for the horizontal and vertical plane are presented on two consecutive lines.

8.1 Fourier Analysis of Tracking Results

The tune shifts can be obtained from tracking by Fourier analysis of the motion. Since the motion is normally only sampled on a turn-by-turn basis, the Discrete Fourier Transform (DFT) has to be used. Since tracking is done for about 512 turns (N), some kind of interpolation must be applied to get a better accuracy than $1/(2N)$.

The DFT is defined by

$$X_n = \frac{1}{N}\sum_{k=0}^{N-1} x_k e^{-i2\pi k\Delta t\, kn/N}, \qquad n = 0, 1, \ldots, N-1 \tag{8.1}$$

and the inverse transform by

$$x_k = \sum_{n=0}^{N-1} X_n e^{i2\pi k\Delta t\, kn/N}, \qquad k = 0, 1, \ldots, N-1 \quad , \tag{8.2}$$

where Δt is the time between two samples. The distribution for a peak, centered around the normalized frequency ν, is given by

$$A(k) = \left|\frac{\sin[\pi(k - N\nu)]}{\pi k}\right|, \qquad k = 0, 1, 2, \ldots, N-1 \tag{8.3}$$

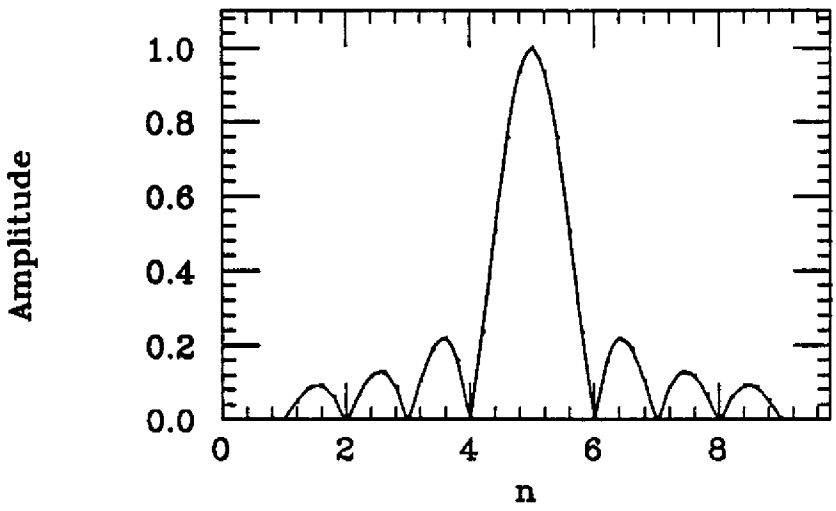

Figure 7: Rectangular window

shown in Figure 7. Note that the DFT is only defined for n = integer. From Eq. (8.3) it is possible to derive the following interpolation for the tune.[21]

$$\nu = \frac{1}{N}\left[k - 1 + \frac{A(k)}{A(k-1) + A(k)}\right], \qquad k - 1 \leq N\nu \leq k \quad . \tag{8.4}$$

We have used a sine window to decrease the sidelobes of a peak in the spectrum. This is done by multiplying the samples x_k by a weight function, in this case

$$y_k = x_k \sin\left(\frac{\pi k}{N}\right), \qquad k = 0, 1, 2, ..., N-1 \tag{8.5}$$

leading to the following distribution for a peak

$$A(k) = \left|\frac{\sin[\pi(k - 1/2 - N\nu)]}{2\pi(k - 1/2 - N\nu)(k + 1/2 - N\nu)}\right|, \qquad k = 0, 1, 2, ..., N-1 \tag{8.6}$$

shown in Figure 8.

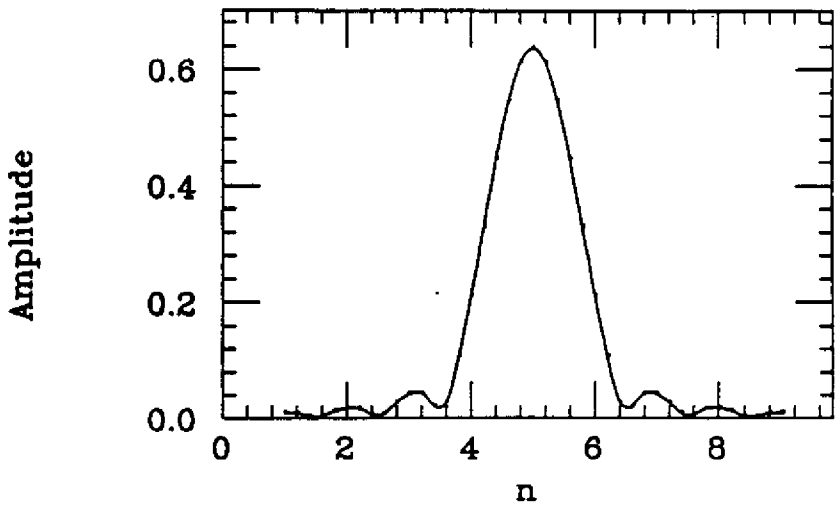

Figure 8: Sine window

We now have[21]

$$\nu = \frac{1}{N}\left[k - 1 + \frac{2A(k)}{A(k-1) + A(k)} - \frac{1}{2}\right] , \qquad k - 1 \leq N\nu \leq k \quad . \tag{8.7}$$

When the tune is known, Eq. (8.6) can be used to obtain the amplitude of a peak.

Smear is obtained by calculating the change of the action variable J defined by Eq. (2.9) using the values from the linear lattice calculations as estimates for the alpha and the beta functions. The rms value of J is then estimated from

$$\sigma_{J_x}^{*2} = \frac{1}{N-1}\sum_{i=1}^{N}(\bar{J}_x^* - J_x)^2 \quad . \tag{8.8}$$

where

$$\bar{J}_x^* = \frac{1}{N}\sum_{i=1}^{N} J_x \quad . \tag{8.9}$$

Another possibility is to Fourier analyze J. The zeroth harmonic gives the average value of J. The average value is then subtracted from the samples, and the rms value of ΔJ is then given by

$$\sigma_{J_x}^{*2} = \sum_{k=0}^{N-1} \frac{A^2(k)}{2} \quad . \tag{8.10}$$

This method has the advantage that the contributions from different multipoles can be resolved. It is done by noticing that to first order the multipoles a_2 , b_2 , a_3 and b_3 in the multipole strength only excite different nonlinear amplitude resonances. These can be identified by fitting a linear combination of the horizontal and vertical tune to each peak in the spectrum. The contribution to the smear for a given multipole is then obtained by restricting the sum to the relevant peaks. A typical example is shown in Figure 9.

8.2 Smear due to random multipoles

Tracking has been done with random errors only for a lattice with 6 dipoles per half cell and 1 TeV injection energy.[22] The amplitudes were

$$A_x = 5.00\,\mathrm{mm}, \qquad A_y = 5.13\,\mathrm{mm} \quad . \tag{8.11}$$

The smear was obtained as averages over 100 seeds. We therefore expect the agreement to be of the order of

$$\pm\sigma_{\bar{S}} = \pm\frac{\sigma_S}{\sqrt{100}} \quad , \tag{8.12}$$

which clearly is the case. The results are shown in Table 16.

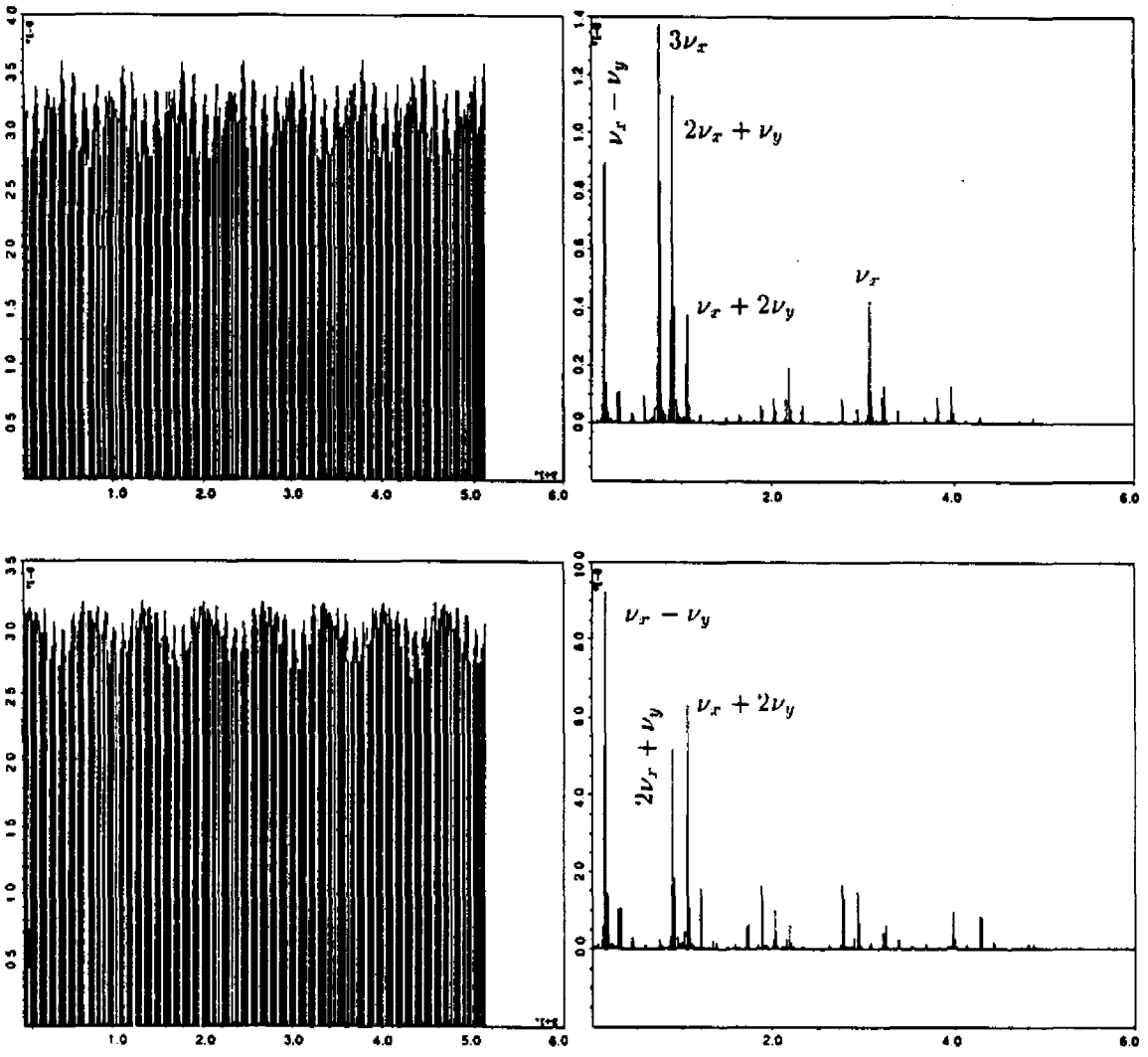

Figure 9: Amplitude resonances

Table 16: Average smear due to random multipoles

a_2	b_2	a_3	b_3	total
1.56(1.50±0.6)	0.87(0.86±0.3)	3.03(2.96±1.4)	0.71(0.66±0.3)	3.62±1.2(3.49±1.6)
1.11(1.05±0.4)	0.99(0.95±0.4)	2.87(2.87±1.3)	0.75(0.68±0.3)	3.39±1.1(3.27±1.4)

A histogram for the total horizontal and vertical smear square, due to the definition of Eq. (2.2), obtained from the tracking is shown in Figures 10 and 11.

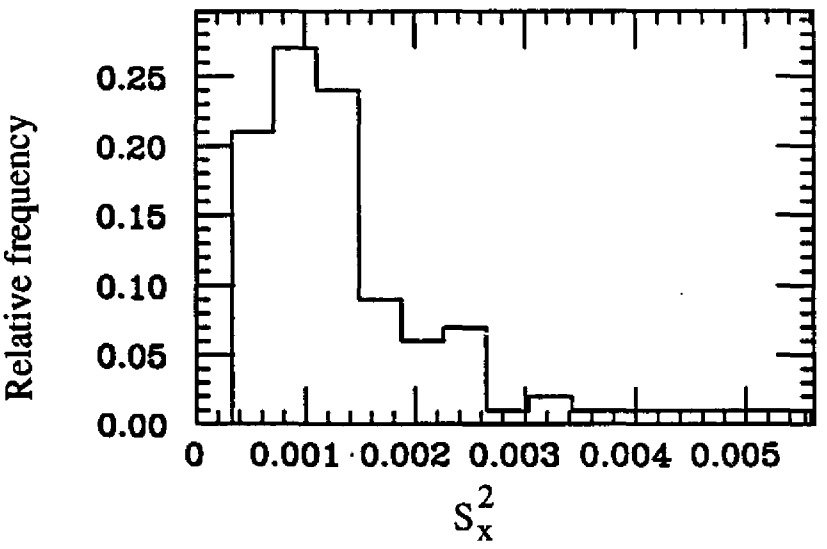

Figure 10: Histogram for the horizontal smear

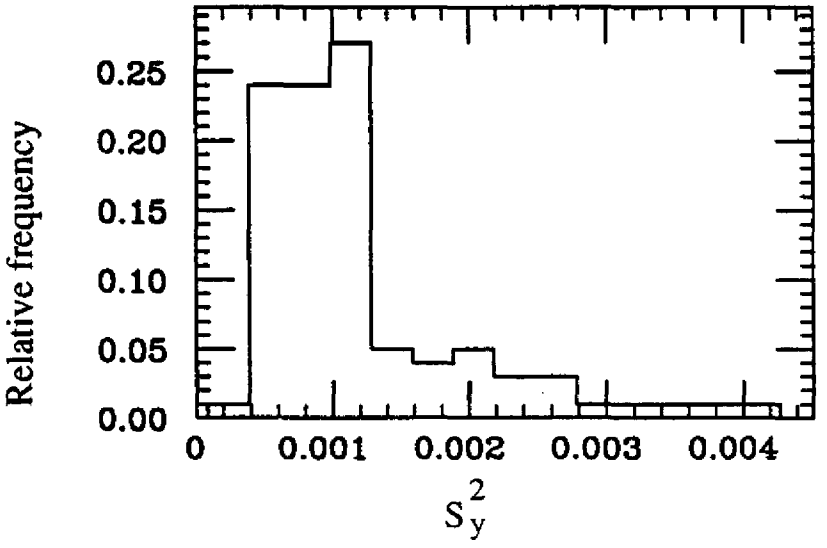

Figure 11: Histogram for the vertical smear

8.3 Smear and Tune Shifts due to Systematic Multipoles

From Table 4-1 in Ref. [23] we have the following results

Table 17:

$A_x = A_y$ (mm)	b_2	$\Delta\nu$ (10^{-3})
5	-4.7	2.5(2.2)
		2.1(2.0)

and from page 18 in Ref. [1], we find

Table 18:

A_x (mm)	A_y (mm)	$\Delta\nu$ (10^{-3})
5	5	5.7(5.7)
		5.8(5.3)
5	0	3.5(3.7)
		2.0(2.0)
		3.7(3.3)
0	5	2.2(2.0)

for

$$b_2 = -7.4\,, \qquad b_3 = 0.1\,, \qquad b_4 = 0.64 \tag{8.13}$$

and the "SNEUFF" correction scheme. We have checked by tracking with TEAPOT that uncorrected systematic a_4 and b_4 give negligible contributions. For the case with 6 dipoles, 1 TeV and 4 cm magnet aperture, we found the contribution to be

$$\begin{aligned} S_x &= 0.01\,\%\,, \qquad \Delta\nu_x = 0.01 \cdot 10^{-3} \\ S_y &= 0.01\,\%\,, \qquad \Delta\nu_y = 0.01 \cdot 10^{-3} \end{aligned} \tag{8.14}$$

In addition, we found that the second order contribution from uncorrected systematic b_2 to the smear are

$$b_2 = -8.4\,, \qquad S_x = 0.12\,\%\,, \qquad S_y = 0.12\,\% \tag{8.15}$$

for an amplitude of

$$\mathrm{A_x} = \mathrm{A_y} = 5.0\,\mathrm{mm} \quad . \tag{8.16}$$

This is quite negligible. However, since this contribution is octupole-like, it will interfere with the contribution from systematic b_3. This explains the discrepancy for the uncorrected systematic b_3 contributions in Table 19. Tracking has also been done for some of the cases in Table 1. The results are shown in Tables 19 and 20.

Table 19: 6 dipoles, 1 TeV, 4 cm magnet aperture

smear (%)	a_2	b_2	a_3	b_3	total
due to systematic multipoles	0.05(0.02) 0.02(0.02)	1.04(1.05) 0.50(0.51)	0.09(0.08) 0.06(0.06)	0.12(0.19) 0.11(0.18)	1.05(1.07) 0.52(0.55)
due to corrected systematic multipoles	0.01(0.01) 0.00(0.00)	0.50(0.51) 0.26(0.27)	0.02(0.01) 0.01(0.01)	0.02(0.00) 0.02(0.00)	0.50(0.51) 0.26(0.27)
$\Delta\nu\,(10^{-3})$					total
due to systematic multipoles					20.9(21.0) 27.3(28.4)
due to corrected systematic multipoles					6.3(6.5) 6.4(6.1)

Table 20: 4 dipoles, 1 TeV, 4 cm magnet aperture

smear (%)	a_2	b_2	a_3	b_3	total
due to corrected	0.00(0.00)	0.30(0.30)	0.01(0.01)	0.02(0.00)	0.30(0.30)
systematic multipoles	0.00(0.00)	0.26(0.26)	0.01(0.01)	0.01(0.00)	0.26(0.26)
$\Delta\nu\,(10^{-3})$					total
due to corrected					1.9(1.8)
systematic multipoles					1.7(1.5)

8.4 Closed Orbit Distortions

The analytically calculated rms orbit has been compared with values obtained from TEAPOT data. [24] Since the corrected orbit is uncorrelated between different cells, the rms orbit was obtained by averaging over the 320 cells of a particular lattice. We have studied the case with one corrector and one bpm per cell for each plane with

$$\Delta x_{\mathrm{quad}}^{\mathrm{rms}} = 0.50\,\mathrm{mm}\,, \qquad \Delta x_{\mathrm{bpm}}^{\mathrm{rms}} = 0.71\,\mathrm{mm}\quad . \tag{8.17}$$

The result is shown in Figure 12 where a dotted line represents the analytically calculated horizontal orbit, a dash represents the corresponding TEAPOT data, a dotdash represents the analytical vertical orbit, and a solid represents the corresponding TEAPOT data. The agreement is quite good, except for a small systematic error in the vertical plane. It is not clear why this error appears. One would expect the two planes to be symmetric as the analytical calculation indicates. In any case, this discrepancy is negligible for the smear calculations.

Since the actual correction scheme for the SSC uses two bpm's per cell, [25] we have compared the analytical calculations, which are based on one bpm with this case, using

$$\Delta x_{\mathrm{quad}}^{\mathrm{rms}} = 1.00\,\mathrm{mm}\,, \qquad \Delta x_{\mathrm{bpm}}^{\mathrm{rms}} = 1.41\,\mathrm{mm}\quad . \tag{8.18}$$

As can be seen from Figure 13, it does not lead to any significant change. This is explained by the fact that the corrected orbit is dominated by the bpm errors, and the best that can be achieved is to make the corrected orbit pass through the center of the bpm's.

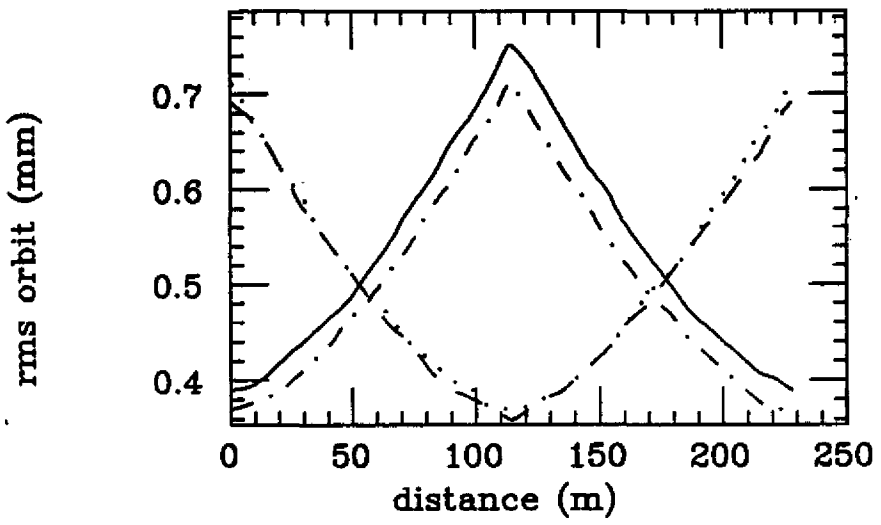

Figure 12: Closed orbit distortions

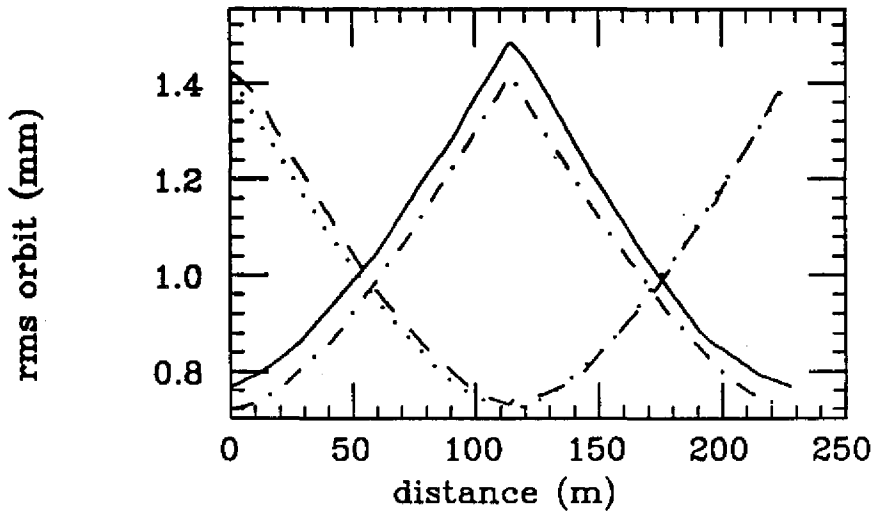

Figure 13: Closed orbit distortions

9. Summary and Conclusions

We have applied and generalized the Lie algebraic formalism developed by E. Forest to calculate smear and tune shifts due to random and systematic multipole errors for the SSC.

It is clear that the presented analytical expressions for the average smear, the spread of the smear, and the tune shifts reproduce in detail the tracking results. By using analytical techniques, the computation times are reduced from hours on the CRAY to seconds on the VAX. Contributions of various multipoles and closed orbit distortions and dependence on amplitude, momentum, and working point are also clear.

The spread of the smear, typically 40%, should be considered so that a specified set of parameters will yield the desired linearity.

This study has been limited to the on-momentum case. To be complete, the off-momentum contributions have to be included.

ACKNOWLEDGEMENTS

We would like to thank A. Chao for his support and overall guidance during this work. We would also like to thank the following people for many helpful discussions and suggestions: E. Forest and J. M. Peterson. Finally, we would like to thank S. Dutt for comments on how to improve the manuscript and V. Kelly for her assistance during the typing of this document.

REFERENCES

1. Correction Element Working Group, *Compensation of SSC Lattice Optics in the Presence of Dipole Field Errors*, SSC-SR-1038.
2. E. Forest and J. M. Peterson, *Correction of Random Multipole Errors with Lumped Correctors*, SSC-N-383.
3. M. A. Furman and S. G. Peggs, *A Standard for the Smear*, SSC-N-634.
4. E. Forest, *Analytical Computation of the Smear*, SSC-95.
5. J. Bengtsson, *Nonlinear Transverse Dynamics for Storage Rings with Applications to the Low Energy Anti-Proton Ring (LEAR) at CERN*, CERN 88-05.
6. K. Y. Ng and N. Merminga, *Analytic Expressions for the Smear due to Nonlinear Multipoles*, SSC-N-594.
7. E. D. Courant and H. S. Snyder, *The Theory of the Alternating-Gradient Synchrotron*, Annals of Physics, **3** (1958) 1.
8. E. Forest, *Computation of First Order Tune Shifts*, SSC-N-322.
9. A. Jackson, *Tune Shifts and Compensation from Systematic Field Components*, SSC-107.
10. SSC Central Design Group, *Conceptual Design Report*, SSC-SR-2020.
11. Parameters Working Group Report, *Magnetic Errors in the SSC*, SSC-7.
12. A. A. Garren and D. E. Johnson, *The 90-Degree (September 1987) SSC Lattice*, SSC-146.
13. A. Dragt, *Lectures on Nonlinear Orbit Dynamics*, Am. Inst. Phys. Conf. Proc. No. 87. R.A. Carrigan et al. (eds.), New York: AIP(1982) 147.
14. E. Forest, *Hamiltonian-Free Perturbation Theory: The Concept of Phase Advance*, SSC-111.
15. *MACSYMA Reference Manual*, Symbolics Inc. (1983).

16. J. P. Delahaye and J. J. Jager, *Variation of the Dispersion Function, Momentum Compaction Factor, and Damping Partition Numbers with Particle Energy Deviation*, Part. Accel. **18** (1986) 183.

17. E. Forest and J. M. Peterson, private communication.

18. J. Peterson, private communication.

19. L. Schachinger, T. Sun, and R. Talman, *Manual for the Program TEAPOT, Noninteractive Version*, unpublished.

20. J. Clement, *TOPDRAWER, Bonner Lab version*, Bonner Lab, Rice University, Houston, Texas.

21. E. Asseo, *Moyens de Calcul pour la Mesure des Force et Phase des Effets Pertubateurs des Résonances sur le Faisceau*, CERN/PS/LEA Note 87-1 (1987).

22. T. Sun, private communication.

23. D. Neuffer and R. Talman, *Comparison of Numerical and Analytical Results for the Systematic Tune Variation of Various Lumped Compensation Schemes for the SSC*, SSC-N-492.

24. L. Schachinger, private communication.

25. A. W. Chao and S. G. Peggs, *Orbit Correction in the Long Arcs of the SSC*, SSC-48.